Optimized domain decomposition methods for the spherical Laplacian

Loisel, Sébastien; Côté, Jean; Gander, Martin Jakob; Laayouni, Lahcen; Qaddouri, Abdessamad

How to cite

LOISEL, Sébastien et al. Optimized domain decomposition methods for the spherical Laplacian. In: SIAM journal on numerical analysis, 2010, vol. 48, n° 2, p. 524–551. doi: 10.1137/080727014

This publication URL: https://archive-ouverte.unige.ch/unige:6259
Publication DOI: 10.1137/080727014

Optimized domain decomposition methods for the spherical Laplacian

S. Loisel * J. Côté † M. J. Gander* L. Laayouni ‡ A. Qaddouri†

September 21, 2009

Abstract

The Schwarz iteration decomposes a boundary value problem over a large domain Ω into smaller subproblems by iteratively solving Dirichlet problems on a cover $\Omega_1, ..., \Omega_p$ of Ω. In this paper, we discuss alternate transmission conditions that lead to faster convergence for the Laplacian on the sphere Ω. We look at Robin conditions, second order tangential conditions and a discretized version of an optimal but nonlocal operator.

1 Introduction

At the heart of numerical weather prediction algorithms lie a Laplace and positive definite Helmholtz problems on the sphere [35]. Recently, there has been interest in using finite elements [5] and domain decomposition methods [4, 26]. The Schwarz iteration [23, 24, 25] and its optimized variants have been very successful and the subject of much recent research. We now outline the history of Optimized Schwarz Methods (OSM) and refer to [14] for further details, as well as a complete derivation for Helmholtz and Laplace problems in the plane.

The optimized Schwarz method was introduced in [2, 31, 32] under various names. Since the OSM has one or more free parameters, which need to be chosen carefully to guarantee the best convergence rate, there followed an effort to find the best possible parameter choices [13, 21, 20]. Despite these positive developments, a proof of convergence for a general situation has proven elusive [22, 27]. One way of obtaining convergence is to define a relaxation of the method [7].

The usual method for optimizing the free parameters is to take a Fourier transform of the partial differential equation, obtaining an explicit recurrence relation for the iteration. This works only in special cases (e.g., the domain is a rectangle and the differential operator is the Laplacian with homogeneous Dirichlet conditions). In addition to the Laplace and Helmholtz problems [19], the method can be used for various other canonical problems (cf. [9, 18, 17, 29, 28] for convection-diffusion problems, [16] for the wave equation, [8] for fluid dynamics, [33] for the shallow water equation). The current paper is a continuation of this research.

Our paper provides an OSM for the spherical Laplacian, a differential operator which had previously not been analyzed, using Fourier analysis. However, we briefly mention that there has been much recent research on various other aspects of the OSM. For instance, domains with corners can give rise to singularities, and this is analyzed in [3]. In a similar vein, differential operators with discontinuous coefficients often lead to ill-conditioned problems, and an OSM for this situation is provided in [12]. A completely different issue is to phrase the OSM in an algebraic way. In a typical application, one has a code to compute the stiffness matrix A, but one would ideally prefer not to have to rewrite the entire code in order to implement an OSM. In that vein, [34] provides a framework for expressing the OSM in the language of matrices.

*Section de Mathématiques, Université de Genéve, CP 64, CH-1211 Geneva, Switzerland (sloisel@gmail.com, gander@math.unige.ch).

†Recherche en prévision numérique, Environnement Canada, 2121 Route Transcanadienne, Dorval, Québec, Canada H9P 1J3 (jean.cote@ec.gc.ca, abdessamad.qaddouri@ec.gc.ca)

‡School of Science and Engineering Al Akhawayn University Avenue Hassan II, 53000 P.O. Box 2165, Ifrane, Morocco (L.Laayouni@aui.ma)

There are many reasons to use domain decomposition methods, but we outline one application. Domain decomposition methods are often naturally parallel, and hence can be used on large clusters and supercomputers. The algorithm that runs on each processor is a small, local version of the global problem, so proven sequential codes can be adapted and become local solvers which will then run in parallel on such clusters. In such a scenario, an important question is that of scaling.

In the simplest scaling scenario, one fixes the number p of subdomains, and one picks subdomains $\Omega_1, \ldots, \Omega_p$ in such a way that the overlap between adjacent subdomains is exactly one element thick. In this situation, it is well known [36] that the (1-level) Schwarz method has a convergence factor of $\rho_{CS} = 1 - O(h)$. In other words, at each step of the iterative method, the error is multiplied by the coefficient $\rho_{CS} < 1$. Because this coefficient depends on h, and tends to 1 when h tends to zero, we see that more and more iterations will be needed to reach a given tolerance as we make h smaller. It is preferable to find an algorithm whose convergence factor either does not approach 1, or at least approaches 1 not too quickly when h tends to zero.

In this context, the main advantage of the Optimized Schwarz methods is that they have much better convergence factors than the classical Schwarz method. For example, the one-sided overlapping OO0 method has a convergence factor of $\rho_{OO0} = 1 - O(h^{1/3})$, and the overlapping OO2 method has a convergence factor of $\rho_{OO2} = 1 - O(h^{1/5})$.

In addition to overlapping methods, Lions [25] proposed to use Robin transmission conditions along the interface to obtain nonoverlapping domain decomposition methods. There is no nonoverlapping classical Schwarz method with which to compare, but the OO0 and OO2 methods can be used in the nonoverlapping context. The convergence factors are $1 - O(h^{1/2})$ and $1 - O(h^{1/4})$, for the nonoverlapping OO0 and OO2 methods, respectively.

Although our analysis is limited to latitudinal subdomains, we will see in Section 5 that we obtain very good performance, even when subdomains have more varied shapes.

We note that, if the number of subdomains p increases as h tends to zero, it is necessary to design a 2-level algorithm to maintain good performance. In a 2-level algorithm, detailed informations from neighbors are combined with less precise information stored on a low-resolution "coarse grid". The design and analysis of an Optimized Schwarz Method with a coarse grid correction is a challenging problem which will be analyzed in an upcoming paper [10].

1.1 Our contributions

In this paper, we introduce improved transmission operators for the Laplace problem on the unit sphere Ω in $\mathbb{R}^3$. We modify the Schwarz iteration by replacing the Dirichlet conditions on the interfaces by Robin or second order tangential conditions. This allows us to significantly improve the convergence factor of the iteration. To analyze the convergence rate and optimize the coefficients, we use the Fourier transform on the sphere. In addition to the usual Robin and second order tangential conditions, we also discuss the use of a nonlocal operator along the interfaces. This nonlocal operator is related to the square root of the Laplacian of the interfaces and was first introduced for numerical calculations in [4, 26]. While the continuous analysis shows that these operators result in an iteration that converges in two steps, in practice we do not see this exact behavior. However, the resulting iteration seems to converge at a very fast rate that is independent of the mesh size h or the thickness of the overlap L.

We highlight four contributions of this paper. First, we have an innovative use of the envelope theorem to establish an equioscillation property. Second, we highlight our continuous and discrete analyses and their comparison. Third, our analysis takes place on the sphere, which is ideal for weather and climate simulation. Fourth, we provide a finite element method which is appropriate for spherical discretizations. Since the spherical Laplacian is singular, the choice of the finite element space is important and a poor choice leads to divergent iterations and poorly conditioned systems. We show that with the proper choice of basis functions, the convergence factor of the optimized Schwarz methods are unaffected.

This paper is organized as follows. In Section 2, we introduce our model problem and state our main results. In Section 3, we review the Laplace operator on the sphere and recall the Schwarz iteration and its convergence estimates, previously published in [4]; we also give a new semidiscrete estimate which is substantially similar to the continuous one. In section 4, we perform the Fourier analysis of the new Optimized Schwarz Methods. In section 5, we present numerical results that agree with the theoretical predictions.

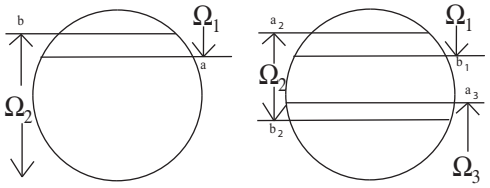

Figure 1: Latitudinal domain decomposition. Left: two subdomains; right: multiple subdomains.

2 OSM on the sphere

Consider the following iteration. Let $b < a$. Begin with random "candidate solutions" u_0 and v_0. Define u_{k+1} and v_{k+1} iteratively by:

$$\left\{\begin{array}{rcll} \Delta u_{k+1} & = & f & \text{in } \Omega_1 = \{(\varphi,\theta)|0 \le \varphi < a\}, \\ u_{k+1}(a,\theta) & = & v_k(a,\theta) & \theta \in [0,2\pi), \\ \Delta v_{k+1} & = & f & \text{in } \Omega_2 = \{(\varphi,\theta)|b < \varphi \le \pi\}, \\ v_{k+1}(b,\theta) & = & u_k(b,\theta) & \theta \in [0,2\pi); \end{array}\right. \tag{1}$$

(see figure 1.) This is the Schwarz iteration for two latitudinal subdomains. The idea of the Optimized Schwarz Methods is to replace the Dirichlet conditions on the interface by Robin or other transmission conditions. The modified iteration is:

$$\left\{\begin{array}{rcll} \Delta u_{k+1} & = & f & \text{in } \Omega_1 \\ ((\psi + \frac{\partial}{\partial\varphi})u_{k+1})(a,\theta) & = & ((\psi + \frac{\partial}{\partial\varphi})v_k)(a,\theta) & \theta \in [0,2\pi), \\ \Delta v_{k+1} & = & f & \text{in } \Omega_2 \\ ((\xi + \frac{\partial}{\partial\varphi})v_{k+1})(b,\theta) & = & ((\xi + \frac{\partial}{\partial\varphi})u_k)(b,\theta) & \theta \in [0,2\pi); \end{array}\right. \tag{2}$$

where ψ and ξ are either real coefficients or trace operators, and Ω_1, Ω_2 are as previously defined. If ψ and ξ are differential trace operators of order k, we say that the optimized Schwarz method is Optimized of Order k, or OOk [15]. Choices include:

1. $(\psi w)(\theta) = cw(\theta)$ where c is a real coefficient. This results in a Robin or OO0 transmission condition.
2. $(\psi w)(\theta) = cw(\theta) + dw''(\theta)$, where c and d are real coefficients. This results in a second order tangential, or OO2 transmission condition.
3. A nonlocal choice of ψ leading to an iteration that converges in two steps.

We will show in Section 3 that the convergence factor depends on the thickness of the overlap L, given by

$$L \quad := \quad -2\log\frac{1+\cos a}{\sin a}\frac{\sin b}{1+\cos b} \ge 0.$$

Our main result for Robin (or OO0) transmission conditions is as follows.

Theorem 2.1 (Optimized Robin or OO0 coefficients)**.** *Consider the iteration (2) with $(\psi w)(\theta) = cw(\theta)$ and $(\xi w)(\theta) = dw(\theta)$. Set $x = -d\sin b$, $y = c\sin a$. Let $h = 1/N$ be the grid size.*

- *The* one-sided condition *is $x = y$. With this condition, and further assuming that $L < 4/3$ and $L > h^\alpha$ for some $\alpha < 3/2$, there is a unique optimized choice of x leading to the best possible convergence factor. Using $x = y = \hat{x}_1 = L^{-\frac{1}{3}}$, the convergence factor every other step is $\rho = 1 - 4L^{\frac{1}{3}} + O(L^{\frac{2}{3}})$.*
- *If $x \neq y$ is allowed, the optimized choice (c,d) is* two-sided*. Assume that $L > h^\alpha$, $\alpha < 5/4$. There is a unique (c,d) leading to the best convergence factor. Using $x = 8^{-\frac{1}{5}}L^{-\frac{1}{5}}$ and $y = \frac{8^{\frac{2}{5}}}{2}L^{-\frac{3}{5}}$ leads to a convergence factor of $\rho = 1 - 2\cdot 2^{\frac{3}{5}}L^{\frac{1}{5}} + O(L^{\frac{2}{5}})$ every other step.*

The convergence factor $\rho < 1$ multiplies the L^2 error of the trace on each subdomain every other step. We see that using "asymmetric" Robin conditions leads to an improvement on the number of iterations required for a given tolerance, from $O(L^{-\frac{1}{3}})$ to $O(L^{-\frac{1}{5}})$. The one-sided estimate however is easier to use with p subdomains, and so we would be interested in achieving a $O(L^{-\frac{1}{5}})$ algorithm using only one-sided estimates. This is possible if we use second order tangential transmission conditions.

Theorem 2.2 (One-sided second order tangential, or OO2, optimized coefficients)**.** *Consider the iteration (2) with* $(\psi w)(\theta) = cw(\theta) + dw''(\theta)$, $(\xi w)(\theta) = \tilde{c}w(\theta) + \tilde{d}w''(\theta)$. *Let* $s = c\sin a = -\tilde{c}\sin b$ *and* $t = d\sin a = -\tilde{d}\sin b$, *which is the "one-sided" assumption. Assume that* $L < h^\alpha$, $\alpha < 5/4$. *There is a unique choice of* s, t *leading to the best possible convergence factor. Using* $s = \frac{1}{2}2^{\frac{3}{5}}L^{-\frac{1}{5}}$ *and* $t = \frac{1}{2}2^{\frac{1}{5}}L^{\frac{3}{5}}$ *leads to a convergence factor of* $\rho = 1 - 4\cdot 2^{\frac{2}{5}}L^{\frac{1}{5}} + O(L^{\frac{2}{5}})$ *every other step.*

The converge rate estimates hold even if L is smaller than h^α (e.g., when the grid is highly anisotropic, with $\alpha = 3/2$ or $5/4$, as above), but then the coefficients given may no longer be optimized. An extreme case is when $L = 0$, a nonoverlapping case, and we analyze this case in Section 3.1. The "main" case is $L = O(h)$ and is handled by the Theorems 2.1 and 2.2.

Our numerical examples are based on two different codes. Many codes in meteorology use the discrete Fourier transform in the longitude variable θ to obtain a *semispectral solver*. This solver makes the implementation of our three types of transmission conditions equally easy, for latitudinal interfaces. However, such solvers do not easily handle arbitrarily shaped subdomains, and the grids have singularities at the poles.

Our second code is a finite element solver on the sphere Ω. The variational formulation of the spherical Laplacian leads to integrals on the sphere Ω, and so we must choose piecewise C^1 basis functions for some finite element space on the sphere Ω. We use a standard projection technique to generate spherical elements from piecewise linear elements on a polyhedral approximation of the sphere Ω.

3 The Laplace operator on the sphere Ω

We take the Laplace operator in $\mathbb{R}^3$, given by

$$\Delta u = u_{xx} + u_{yy} + u_{zz},$$

rephrase it in spherical coordinates and set $\frac{\partial u}{\partial r} = 0$ to obtain

$$\Delta u = \frac{1}{\sin^2\varphi}\frac{\partial^2 u}{\partial\theta^2} + \frac{1}{\sin\varphi}\frac{\partial}{\partial\varphi}\left(\sin\varphi\frac{\partial u}{\partial\varphi}\right),$$

where $\varphi \in [0,\pi]$ is the colatitude and $\theta \in [-\pi,\pi]$ the longitude.

3.1 The solution of the Laplace problem

We take a Fourier transform in θ but not in φ; this lets us analyze domain decompositions with latitudinal boundaries. The Laplacian becomes

$$\hat{\Delta}\hat{u}(\varphi,m) = \frac{-m^2}{\sin^2\varphi}\hat{u}(\varphi,m) + \frac{1}{\sin\varphi}\frac{\partial}{\partial\varphi}\left(\sin\varphi\frac{\partial\hat{u}(\varphi,m)}{\partial\varphi}\right),\ \varphi\in[0,\pi],\ m\in\mathbb{Z}. \tag{3}$$

For boundary conditions, the periodicity in θ is taken care of by the Fourier decomposition. The poles impose that $u(0,\theta)$ and $u(\pi,\theta)$ do not vary in θ. For $m \neq 0$ this is equivalent to

$$\hat{u}(0,m) \quad = \quad \hat{u}(\pi,m) = 0,\ m\in\mathbb{Z},\ m\neq 0. \tag{4}$$

For $m = 0$, the relation $u_\varphi(0,\theta) = -u_\varphi(0,\theta+\pi)$ leads to $\int_0^{2\pi} u_\varphi(0,\theta)\,d\theta = -\int_0^{2\pi} u_\varphi(0,\theta)\,d\theta$, i.e.,

$$\hat{u}_\varphi(0,0) \quad = \quad \hat{u}_\varphi(\pi,0) = 0. \tag{5}$$

If u is a solution of $\Delta u = f$ then so is $u + c$ ($c \in \mathbb{R}$), hence the ODE for $m = 0$ is determined up to an additive constant.

With $m \neq 0$ fixed, the two independent solutions of $\Delta u = 0$ are

$$g_\pm(\varphi, m) = \left(\frac{\sin(\varphi)}{\cos(\varphi)+1}\right)^{\pm|m|} = e^{\pm|m|\log\frac{\sin(\varphi)}{\cos(\varphi)+1}},\ m \in \mathbb{Z}\setminus\{0\}.$$

For $m = 0$ the two independent solutions give

$$\hat{u}(\varphi, 0) \quad = \quad C_1 + C_2 \log\frac{1-\cos\varphi}{\sin\varphi}.$$

If we insist, for instance, that $u \in H^1(\Omega)$, we eliminate the logarithmic term and we obtain that $\hat{u}(\varphi, 0)$ is a constant in φ.

All the eigenvalues of Δ are of the form of $-n(n+1)$ for $n = 0, 1, ...$; in particular, they are non-positive (and Δ is negative semi-definite).

3.2 The Schwarz iteration for Δ with two latitudinal subdomains

Consider the Schwarz iteration (1). We are interested in studying the error terms $u_0 - u$ and $v_0 - u$ where $\Delta u = f$. Observe that $u_k - u$ and $v_k - u$ are classical Schwarz iterates as per equation (1), but with $f = 0$. For this reason, it suffices to analyze the classical Schwarz iteration with $f = 0$, which we assume for the remainder of our analysis.

Using the Fourier transform in θ, we can write $\hat{u}_{k+2}(b, m)$ explicitly in terms of $\hat{u}_k(b, m)$. This allows us to obtain a convergence factor estimate, which we recall from [4].

Lemma 3.1. *The Schwarz iteration on the sphere Ω partitioned along two latitudes $b < a$ converges (except for the constant term). The convergence factor $|\hat{u}_{k+2}(b, m)/\hat{u}_k(b, m)|$ is*

$$C(m) = \left(\frac{\sin(b)}{\cos(b)+1}\right)^{2|m|}\left(\frac{\sin(a)}{\cos(a)+1}\right)^{-2|m|} < 1. \tag{6}$$

This convergence factor depends on the frequency m of u_k on the latitude b.

An analysis that is closer to the numerical algorithm would be to replace the continuous Fourier transform in θ by a discrete one.

Lemma 3.2 (Semidiscrete analysis.)**.** *The Laplacian discretized in θ with n sample points:*

$$\Delta_n u = \frac{n^2}{4\pi^2\sin^2\varphi}\left(u\left(\varphi, \frac{j+1}{2\pi n}\right) - 2u(\varphi, j) + u\left(\varphi, \frac{j-1}{2\pi n}\right)\right) + \cot\varphi u_\varphi + u_{\varphi\varphi} \tag{7}$$

leads to a Schwarz iteration whose convergence factor is

$$\left(\frac{\sin(b)}{\cos(b)+1}\right)^{2|\tilde{m}|}\left(\frac{\sin(a)}{\cos(a)+1}\right)^{-2|\tilde{m}|} < 1$$

every two iterations, where

$$\tilde{m}^2 = \frac{n^2}{4\pi^2}(1-\cos(2\pi k/n))$$

for the kth frequency.

Proof. We do a discrete Fourier transform in θ and the equation to solve becomes

$$L_n\hat{u}(\varphi, k) = \frac{n^2}{4\pi^2\sin^2\varphi}(\cos(2\pi k/n) - 1)\hat{u}(\varphi, k) + \cot\varphi\hat{u}_\varphi(\varphi, k) + \hat{u}_{\varphi\varphi}(\varphi, k) = 0. \tag{8}$$

By writing m as noted in the statement of the Lemma, we have reduced this problem to the previous one and we can reuse Lemma 3.1. □

The two contraction constants are very similar. For small values of m (ignoring $m = 0$ because that mode need not converge at all), the speed of convergence is very poor. The overall convergence factor as measured in the L^2 norm along the interfaces is given by

$$\begin{aligned}\sup_{m\geq 1} C(m) &= C(1)\\ &= 1 - O(a-b),\end{aligned}$$

and so the convergence factor of the Schwarz iteration deteriorates rapidly as $a - b$ becomes small.

4 Optimized Schwarz iteration for Δ with latitudinal boundaries

In this section, we prove Theorems 2.1 and 2.2. This requires many technical results and so we proceed with a sequence of simple lemmas.

To analyze the convergence factor, as we did in Section 3, we assume, without loss of generality, that $f = 0$. Because the Laplacian of a constant is zero, we will see that the error terms converge to constant functions, which is to say, the local solutions converge up to an additive constant.

One key technique is to use the fact that, although u_0 and v_0 may be arbitrary in some Sobolev spaces, u_1 and v_1 are harmonic in Ω_1 and Ω_2, respectively. This key observation allows us to find iterations that converge fast *starting from the second step*. This observation has an impact on the numerical simulations. Often, the first iterations u_1 and v_1 are not much better than the initial guesses u_0 and v_0, and they are sometimes even worse.

Lemma 4.1 (Nonlocal operator)**.** *If, for each m, $\hat{\psi}(m) = |m|/\sin a$ and $\hat{\xi}(m) = -|m|/\sin b$, $\Delta u_1 = 0$ in Ω_1 and $\Delta v_1 = 0$ in Ω_2, then $u_2 = 0$ and $v_2 = 0$.*

Proof. Let $u_1(\varphi,\theta) = \hat{u}_1(a,0)+\sum_{k\neq 0}\hat{u}_1(a,k)g_+(\varphi,k)e^{ik\theta}$ and $v_1(\varphi,\theta) = \hat{v}_1(a,0)+\sum_{k\neq 0}\hat{v}_1(a,k)g_-(\varphi,k)e^{ik\theta}$, then the boundary value problem for the north hemisphere yields for each $m \neq 0$:

$$\hat{u}_2(a,m)\left(\hat{\psi}(m) + \frac{|m|}{\sin a}\right) = \hat{v}_1(a,m)\left(\hat{\psi}(m) - \frac{|m|}{\sin a}\right) = 0, \tag{9}$$

and so $\hat{u}_2(a,m) = 0$. Likewise, we find that $\hat{v}_2(b,m) = 0$ for each $m \neq 0$. For $m = 0$, we have that $\hat{u}_2(a,m) = \hat{v}_1(a,m)$: the iteration does not affect the constant mode $m = 0$. Since the solution of the Laplace problem is only defined up to a constant, the iteration has converged. □

The second tangential derivative D_θ^2 along latitude φ has Fourier transform $-m^2$. The optimal operators are therefore the symmetric and positive definite square root of $-D_\theta^2$, multiplied by $1/\sin a$ or $1/\sin b$ according to the latitude. This normalization constant is related to the length of the latitude at $\varphi = a$ and $\varphi = b$, respectively, since a latitude φ is a circle of radius $r = \sin\varphi$.

Next, we state the convergence factor of the optimized Schwarz iteration, if ψ and ξ are not these nonlocal operators.

Lemma 4.2. *If $\Delta u_1 = 0$ in Ω_1 then*

$$\hat{u}_3(b,m) \quad = \quad \hat{u}_1(b,m)\frac{\hat{\xi}(m)\sin b + |m|}{\hat{\xi}(m)\sin b - |m|}\frac{\hat{\psi}(m)\sin a - |m|}{\hat{\psi}(m)\sin a + |m|}\frac{g_-(m,a)}{g_-(m,b)}\frac{g_+(m,b)}{g_+(m,a)}.$$

The proof is a simple computation using equation (9). We now look for good convolution kernels ξ and ψ so that the the convergence factor

$$\kappa(\psi,\xi,m,a,b) \quad = \quad \overbrace{\frac{\hat{\xi}(m)\sin b + |m|}{\hat{\xi}(m)\sin b - |m|}}^{\kappa_1}\overbrace{\frac{\hat{\psi}(m)\sin a - |m|}{\hat{\psi}(m)\sin a + |m|}}^{\kappa_2}\overbrace{\frac{g_-(m,a)}{g_-(m,b)}}^{\kappa_3}\overbrace{\frac{g_+(m,b)}{g_+(m,a)}}^{\kappa_4}, \tag{10}$$

with $m \in \mathbb{Z}\setminus\{0\}$, is as small as possible. For a given choice of $\hat{\psi}$ and $\hat{\xi}$, the convergence factor as measured in the L^2 norm along the interface $\varphi = b$ will be given by $\sup_{m\in\mathbb{Z}\setminus\{0\}}|\kappa(\psi,\xi,m,a,b)|$.

The convergence factor estimate (10) also leads to the following result:

Corollary 4.3. *The iteration (2) is convergent (modulo the constant mode) if ψ and $-\xi$ are convolution operators that are positive definite, regardless of overlap.*

Proof. Let $\hat{\psi}(m) > 0$ and $\hat{\xi}(m) < 0$, and let $\kappa_1, \kappa_2, \kappa_3, \kappa_4$ be as in (10). Since $\sin a > 0$ and $\sin b > 0$, we see that $|\kappa_1| < 1$ and $|\kappa_2| < 1$. Furthermore,

$$\kappa_3\kappa_4 = \left(\frac{\sin(b)}{\cos(b)+1}\right)^{2|m|}\left(\frac{\sin(a)}{\cos(a)+1}\right)^{-2|m|} = \left(\overbrace{\left(\frac{\sin(b)}{\sin(a)}\right)}^{\leq 1}\overbrace{\left(\frac{\cos(a)+1}{\cos(b)+1}\right)}^{\leq 1}\right)^{2|m|} \leq 1,$$

where we have used that $b < a$. Hence, $|\kappa(\psi,\xi,m,a,b)| < 1$ for every $m \neq 0$. □

By comparison, in [27], it was shown that if ξ and ψ are Robin transmission conditions for a domain decomposition with "relatively uniform overlap", then the iteration converges so long as ξ and ψ are both positive definite.

Our analysis will proceed by considering the contraction constant (10) for the various choices of transmission conditions ξ and ψ. We consider first the use of Robin transmission conditions and prove Theorem 2.1. Second, we prove Theorem 2.2 for second order tangential transmission conditions.

4.1 Robin or OO0 transmission conditions

Let $\psi u = cu$ and $\xi u = du$, then

$$\begin{aligned}\kappa_{OO0}(\psi,\xi,m,a,b) &= \frac{d\sin b+|m|}{d\sin b-|m|}\frac{c\sin a-|m|}{c\sin a+|m|}\frac{g_-(m,a)}{g_-(m,b)}\frac{g_+(m,b)}{g_+(m,a)}\\ &= \kappa(c,d,m,a,b).\end{aligned}$$

For a, b fixed, we now need to compute the choices of c, d minimizing

$$\varphi(c,d) = \sup_m \kappa_{OO0}(c,d,m,a,b)^2,$$

where we have introduced a square to simplify some calculations; the actual contraction constant will be given by $\sqrt{\varphi(c,d)}$. To simplify our notation, it is convenient to do a change of variables. We set $x = -d\sin b$, $y = c\sin a$ and

$$L = -2\log\left(\frac{1+\cos a}{\sin a}\frac{\sin b}{1+\cos b}\right) \geq 0,$$

and rewriting the $g_\pm$ terms as exponentials, the optimization problem becomes

$$\begin{aligned}&&\text{Minimize } \varphi(x,y) \text{ where}\\ \varphi(x,y) &= \sup_{m\in\{1,2,\ldots\}} F(x,y,m)\\ F(x,y,m) &= \left|\frac{x-m}{x+m}\frac{y-m}{y+m}e^{-Lm}\right|^2 \qquad (11)\\ &= F_L(x,y,m).\end{aligned}$$

The convergence factor every other step for particular parameter choices x and y is $\sqrt{\varphi(x,y)}$. The case $L = 0$ only occurs when $a = b$, in which case $\varphi(x,y) = 1$ for all $x, y \geq 1$ and then we will need to take into account certain discretization parameters to obtain a convergence factor estimate. This case will be treated separately.

We now use two different analyses to compute optimized Robin parameters c and d. First, we make the simplifying assumption that $x = y$, allowing us to optimize instead the objective function

$$\max_m |(x-m)/(x+m)e^{-\frac{L}{2}m}|^2.$$

This situation is interesting because this can lead to an algorithm where all subdomains "do the same thing". This is the method which most obviously generalizes to many subdomains. Second, we consider the expression $F(x,y,m)$ with both parameters simultaneously. This is also interesting, because in this situation, the iteration does "something different" on each subdomain. We will see that, although this approach is difficult to generalize to many subdomains, it leads to substantially improved convergence factors.

4.2 OO0 one-sided analysis, $L > 0$.

We can write $F_L(x,y,m) = F_L(x,m)F_L(y,m)$ (cf. (11)), where we define

$$F_L(x,m) = F(x,m) = \left|\frac{x-m}{x+m}e^{-\frac{L}{2}m}\right|^2.$$

We first look at the problem of computing the optimal parameter x_0 minimizing

$$\varphi_L(x) = \sup_{m\in\{1,2,\ldots\}} F_L(x,m),$$

since it is simpler. The solution x_0 minimizing $\varphi_L(x)$ leads to the choices $x = y = x_0$, which minimizes $\varphi_L(x,y)$ subject to the symmetry constraint $x = y$. The convergence factor for a particular parameter choice x is $\sqrt{\varphi(x,x)} = \varphi_L(x)$.

We now deal with the various spectra over which we can optimize. Our continuous problem has a frequency variable $m \in \mathbb{Z}$, but since the $m = 0$ frequency need not converge, and since $F_L(x,-m) = F_L(x,m)$, we have already simplified our problem by considering the frequencies $m \in \{1,2,\ldots\}$. Because of our eventual discretization, we will want to consider the frequency domain $\{1,2,...,N\}$, where N is the highest frequency that can be resolved on the interface, given our grid. However, because of the difficulties in optimizing over discrete sets, we also consider the possibility of allowing m to vary in the intervals $[1,\infty)$ as well as $[1,N]$. For technical reasons, it is also convenient to include $m = \infty$ in our calculations.

Let $2 < N < \infty$ and define

$$\begin{aligned}
\varphi_L^{(c)}(x) &= \sup_{m\in[1,\infty]} F_L(x,m),\ (I^{(c)} = [1,\infty]),\\
\varphi_L^{(d)}(x) &= \sup_{m\in\{1,2,\ldots\}} F_L(x,m),\ (I^{(d)} = \{1,2,...,\infty\}),\\
\varphi_L^{(cb)}(x) &= \sup_{m\in[1,N]} F_L(x,m),\ (I^{(cb)} = [1,N]),\\
\varphi_L^{(db)}(x) &= \sup_{m\in\{1,2,\ldots,N\}} F_L(x,m),\ (I^{(db)} = \{1,2,...,N\}).
\end{aligned}$$

According to our definitions, for all x, $\varphi_L^{(d)}(x) = \varphi_L(x)$. The other functions are similar but maximize over a different set of frequencies.

One of the main tools for solving min-max problems is the envelope theorem, which we state here for convenience.

Theorem 4.4 (The Envelope Theorem)**.** *Let U be open in $\mathbb{R}^n$ and $\varphi : U \to R$, $\gamma \in \mathbb{R}^n$, $||\gamma|| = 1$. For $x \in U$, define the one-sided directional derivative $D_\gamma\varphi(x)$ by*

$$D_\gamma\varphi(x) = \lim_{\epsilon\downarrow 0^+} \frac{\varphi(x+\epsilon\gamma)-\varphi(x)}{\epsilon},$$

if the (one-sided) limit exists. Let V be a compact metric space. Let

$$\begin{aligned}
F : U\times V &\to \mathbb{R}\\
(x,y) &\mapsto F(x,y)
\end{aligned}$$

be continuous and assume that the partial gradient $F_x(x,y)$ exists for all $x,y \in U\times V$ and varies continuously in (x,y). Define

$$\begin{aligned}
\varphi(x) &= \max_{y\in V} F(x,y),\\
Y(x) &= \{y \in V | F(x,y) = \varphi(x)\} \neq \emptyset.
\end{aligned}$$

Then,

1. *For all $x \in U$ and $\gamma \in \mathbb{R}^n$, $||\gamma|| = 1$, $D_\gamma u(x)$ exists and is given by the formula*

$$D_\gamma\varphi(x) = \max_{y\in Y(x)} \sum_{i=1}^n \gamma_i F_{x_i}(x,y). \tag{12}$$

2. *Let $\tilde{x} \in U$. If $Y(\tilde{x}) = \{y(\tilde{x})\}$ is a single point then*

$$D_\gamma\varphi(\tilde{x}) = \sum_{i=1}^n \gamma_i F_{x_i}(\tilde{x},y) \tag{13}$$

and φ is (fully) differentiable at $\tilde{x}$. If furthermore $Y(x) = \{y(x)\}$ is a singleton for all $x \in O \subset U$ an open set, then φ is continuously differentiable in O.

This immediately leads to an equioscillation property.

Lemma 4.5. *For $j \in \{c, d, cb, db\}$, there is a minimizer x_j of $\varphi^{(j)}(x)$, and $|M^{(j)}(x_j)| \geq 2$, where $M^{(j)}(x) = \{m \in I^{(j)} | \varphi^{(j)}(x) = F_L(x, m)\}$.*

Proof. We must place ourselves in the hypotheses of the envelope theorem. Each set $[1, \infty]$, $\{1, 2, ..., \infty\}$, $[1, N]$, $\{1, 2, ..., N\}$ is a compact metric space (for $I^{(c)}$ and $I^{(d)}$ one may use the metric $d(x, y) = |x^{-1} - y^{-1}|$). Since the function $\varphi^{(j)}$ is a continuous function on the compact metric space $I^{(j)}$, it must have a minimum. The optimal parameter x_j is in $[0, \infty)$ so we take $U = (-\frac{1}{2}, \infty)$, and the hypotheses of the envelope theorem are satisfied.

Assume that $M^{(j)}(x_j) = \{\tilde{m}\}$ is a singleton (there is no equioscillation). Then, by the envelope theorem, the two-sided derivative $D_x \varphi^{(j)}(x_j)$ exists and since $\varphi^{(j)}(x_j)$ is minimal, the derivative must be zero. Using formula (13), we obtain

$$0 \quad = \quad F_x(x_j, \tilde{m}) = -4\tilde{m} \frac{\tilde{m} - x_j}{(\tilde{m} + x_j)^3} e^{-2L\tilde{m}}.$$

Since $x_j, \tilde{m} > 0$, it must be that $\tilde{m} = x_j$. Hence, $\varphi^{(j)}(x_j) = F(x_j, \tilde{m}) = 0$. But we know that $\varphi^{(j)}(x_j) \geq F(x, x + 1) > 0$. □

Now we characterize the unique minimizer for the case $j = c$.

Lemma 4.6. *There is a unique x_c minimizing $\varphi_L^{(c)}(x)$ and it is the unique root $\psi(x_c) = 0$ of*

$$\psi(x) \quad = \quad \psi(x, L) = \left(\frac{m(x) - x}{m(x) + x} \right)^2 e^{-Lm(x)} - \left(\frac{1 - x}{1 + x} \right)^2 e^{-L},$$

where $m(x) = \sqrt{\frac{4x}{L} + x^2}$.

Proof. Because any minimizer x_c is in $[1, \infty)$, the only local maxima of $F_L(x, m)$ as m runs in $[1, \infty]$ are at $m = 1$ and $m = m(x) = \sqrt{\frac{4x}{L} + x^2}$ and so $M^{(c)}(x_c) \subseteq \{1, m(x_c)\}$. By Lemma 4.5, we know that $\# M^{(c)}(x_c) \geq 2$ so

$$M^{(c)}(x_c) \quad = \quad \left\{ 1, \sqrt{\frac{4x_c}{L} + x_c^2} \right\}.$$

Hence, $\psi(x_c) = 0$. This shows the equioscillation $\psi(x) = 0$.

We now show the uniqueness of the solution of the equioscillation problem. To that end, let

$$\begin{aligned} g(x) &= F(x, m(x)), \\ g'(x) &= F_x(x, m(x)) + F_m(x, m(x)) m'(x) \\ &= F_x(x, m(x)) \\ &= -4m(x) \frac{m(x) - x}{(m(x) + x)^3} e^{-Lm(x)} < 0, \end{aligned}$$

and

$$\begin{aligned} h(x) &= F(x, 1), \\ h'(x) &= -4 \frac{1 - x}{(1 + x)^3} e^{-L} > 0. \end{aligned}$$

Hence, $\psi' = g' - h' < 0$ and ψ may not have multiple zeros. □

This result gives some more information for the case $j = d$ (that is, $I^{(d)} = \{1, 2, ..., \infty\}$). We must assume that L is not too big, but our focus is the case where there is little overlap so this is not a problem. The special point $m(x)$ continues to play an important role. Notice that $m'(x) > 1$ and that $m(1) = \sqrt{4 + L}/\sqrt{L} > 1$ so that, for all $x > 1$, $m(x) > m(1) + (x - 1) > x$.

Lemma 4.7. *Let $L < 4/3$ and let x_c minimize $\varphi_L^{(c)}(x)$ and x_d minimize $\varphi_L^{(d)}(x)$. Then $1 \in M^{(d)}(x_d) \subseteq \{1, \lceil m(x_d)\rceil, \lfloor m(x_d)\rfloor\}$ and $x_c - 1 \le x_d \le x_c$.*

Proof. Because $m = m(x_d)$ is the only local maximum of $F_L(x,m)$, we know that $M^{(d)}(x_d) \subseteq \{1, \lceil m(x_d)\rceil, \lfloor m(x_d)\rfloor\}$, and we also know from Lemma 4.5 that $\#M^{(d)}(\hat{x}) \ge 2$. Assume that $M^{(d)}(\hat{x}) = \{\lceil m(\hat{x})\rceil, \lfloor m(\hat{x})\rfloor\}$. The hypothesis on L combined with the fact that $x_d \ge 1$ guarantees that $m(x_d) > x_d + 1$ so $x_d < \lfloor m(x_d)\rfloor$. We can now use the one-sided derivative of the Envelope Theorem, obtaining that

$$\begin{aligned} D_{(1)}\varphi^{(d)}(x_d) &= \max_{m\in\{\lceil m(x_d)\rceil, \lfloor m(x_d)\rfloor\}} F_x(x_d, m) \\ &= \max_{m\in\{\lceil m(x_d)\rceil, \lfloor m(x_d)\rfloor\}} -m\frac{m-x_d}{(m+x_d)^3}e^{-Lm} < 0. \end{aligned}$$

Therefore, $1 \in M^{(d)}(\hat{x})$.

Clearly, we must have $\varphi^{(d)}(x_d) \le \varphi^{(c)}(x_c)$. If $x_d > x_c$ then $\varphi^{(d)}(x_d) \ge F(x_d, 1) = \varphi^{(c)}(x_d) > \varphi^{(c)}(x_c)$, hence we must have that $x_d \le x_c$. If $x_d < x_c - 1$, then in view of the estimate $m'(x) > 1$, we have that $m(x_d) < m(x_c) - 1$. Let $m_0 = \lfloor m(x_c)\rfloor$ and find the unique $x_0 \in (1, m_0)$ such that $m(x_0) = m_0$. We have that $x_d \in (1, x_0) \subset (1, m_0)$. For $x \in (1, m_0)$, we have that $F_x(x, m_0) < 0$. Hence, $\varphi^{(d)}(x_d) \ge F(x_d, m_0) > F(x_0, m_0) = \varphi^{(c)}(x_0) > \varphi^{(c)}(x_c)$. ☐

As a result of Lemma 4.7, we see that using the discrete frequency spectrum $\{1, 2, ..., \infty\}$ or using the continuous frequency spectrum $[1, \infty]$ results in approximately the same Robin parameter.

We would like to give a formula for the optimized Robin parameter, but the equioscillation property cannot be solved explicitly. However, we can solve it approximately for small L. This further allows us to consider the spectrum $[1, N]$. If x_{cb} minimizes $\varphi^{(cb)}(x)$ then $M^{(cb)}(x_{cb}) \subseteq \{1, N, m(x_{cb})\}$. When L is not too small compared to N^{-1}, we now show that $M^{(cb)}(x_{cb}) = \{1, m(x_{cb})\}$. This implies that, for those values of L and N, the optimized parameter for the frequency spectrum $[1, N]$ is the same as the one for the frequency spectrum $[1, \infty]$.

Lemma 4.8. *The optimized choice x_c for $\varphi^{(c)}(x_c)$ is asymptotic to $L^{-\frac{1}{3}}$:*

$$\lim_{L\to 0^+} x_c L^{\frac{1}{3}} = 1.$$

If we choose $\hat{x}_c = L^{-\frac{1}{3}}$ as our optimized parameter, the convergence factor every other step is

$$F(\hat{x}_c, 1) = 1 - 4L^{\frac{1}{3}} + O(L^{\frac{2}{3}}). \tag{14}$$

Let $\alpha > -3/2$. If $L = L(N) > N^{\alpha}$ then for all N sufficiently large, $m(x_c) < N$, and for such values of N and L, we have that $x_c = x_{cb}$.

Proof. We try to solve $F(x, m(x)) - F(x, 1) = 0$ by writing x as a power of L. Let $x = CL^{\beta}$, then we get

$$0 = \psi = \left(\frac{\sqrt{CL^{\beta-1} + C^2L^{2\beta}} - CL^{\beta}}{\sqrt{CL^{\beta-1} + C^2L^{2\beta}} + CL^{\beta}}\right)^2 e^{-L\sqrt{4CL^{\beta-1}+C^2L^{2\beta}}} - \left(\frac{1-CL^{\beta}}{1+CL^{\beta}}\right)^2 e^{-L}, \tag{15}$$

which is defined for $L > 0$ and $C > 0$. We want to take a series expansion for ψ, and we find that for $\beta = -1/3$,

$$\psi = \left(\frac{4}{C} - 4\sqrt{C}\right) L^{\frac{1}{3}} + O(L^{\frac{2}{3}}).$$

We see that $G(x) = F(x, m(x)) - F(x, 1) < 0$ for sufficiently small L if we choose $x = CL^{-\frac{1}{3}}$ with $C > 1$, and $G(x) > 0$ for all sufficiently small L if $C < 1$. Hence, $x_c L^{\frac{1}{3}} \to 1$ as $L \to 0^+$.

To show that $x_c = x_{cb}$, it suffices to show that

$$m(x_c) < N, \tag{16}$$

for sufficiently small L. We substitute $x = L^{-\frac{1}{3}}$ and then $L = N^{\alpha}$ into $m(x)$ obtaining

$$m(x) = \sqrt{4N^{-\frac{4}{3}\alpha} + N^{-\frac{2}{3}\alpha}}.$$

Hence if $\alpha > -3/2$, $m(x)/N \to 0$ as $N \to \infty$ and so $m(x) < N$ for large N. Conversely, if $\alpha < -3/2$, $m(x)/N \to \infty$ and $m(x) > N$ for large N. ☐

The case $\{1, 2, ..., N\}$ follows immediately.

Corollary 4.9. *Let $\alpha > -\frac{3}{2}$. Let $L = L(N) > O(N^\alpha)$, $L < \frac{4}{3}$ and let x_{cb} minimize $\varphi^{(cb)}(x)$. If x_{db} minimizes $\varphi^{(db)}(x)$ then for all N sufficiently large, $1 \in M(x_{db}) \subset \{1, \lfloor m(x_c) \rfloor, \lceil m(x_c) \rceil\}$.*

Proof. Say that x_d minimizes $\varphi^{(d)}(x)$. By lemma 4.7, we have that $M^{(d)}(x_d) \subseteq \{1, \lceil m(x_c) \rceil, \lfloor m(x_c) \rfloor\}$, where x_c minimizes $\varphi^{(c)}(x)$. Lemma 4.8 gives $\lceil m(x_c) \rceil < N$ for large N, hence $M^{(d)}(x_d) \subset \{1, ..., N\}$. If $x_{db} > x_d$ then $F(x_{db}, 1) > F(x_d, 1)$ and x_{db} is not a minimizer. If $x_{db} < x_d$ and if $1 \neq m_d \in M^{(d)}(x_d)$ then $\varphi^{(db)}(x_{db}) \geq F(x_{db}, m_d) \geq F(x_d, m_d) = \varphi^{(d)}(x_d)$ and x_{db} is not a minimum. Hence $x_d = x_{db}$ for all sufficiently large N. □

Note that the asymptotic convergence factor (14) is approximately independent of the spectrum we use, and so we may use the optimized parameter $\hat{x}_c = L^{-\frac{1}{3}}$ in all situations.

This completes the proof of the first part of Theorem 2.1.

4.3 Two-parameter OO0 analysis, $L > 0$.

Returning to formula (11), we now compute the optimal parameters x and y without assuming that $x = y$. Calculations in this setting are more complicated than in the one-parameter case, so we treat only the cases of the spectrum $[1, \infty]$ and $[1, N]$. We can get a rudimentary equioscillation property out of the envelope theorem.

Lemma 4.10. *Let $L > 0$ and*

$$\begin{aligned} F(x, y, m) &= \left(\frac{x - m}{x + m} \frac{y - m}{y + m} e^{-Lm} \right)^2, \\ \varphi(x, y) &= \sup_{m \in [1, \infty]} F(x, y, m), \\ M(x, y) &= \{m \in [1, \infty] | F(x, y, m) = \varphi^{(j)}(x, y)\}. \end{aligned}$$

Then $\varphi(x, y)$ has a minimum (x_0, y_0). In addition, $\#M^{(j)}(x_0, y_0) \geq 2$ and $\min(x_0, y_0) \geq 1$.

Proof. Note that $\varphi(1, 1) < 1$. Since $\varphi(x, y) \geq F(x, y, 1)$ and since $F(x, y, 1)$ tends to 1 as (x, y) tends to ∞, there is an $M < \infty$ such that, if $(x, y) \notin [1, M] \times [1, M]$, then $\varphi(x, y) > \varphi(1, 1)$. Hence, φ must have a minimum in $[1, M] \times [1, M]$.

We now place ourselves under the hypotheses of the Envelope Theorem. We have that $(x_0, y_0) \in (\frac{1}{2}, \infty)^2 = U$ and the choice $V = [1, \infty]$ does the trick.

If $M^{(j)}(x_0, y_0) = \{m\}$ is a singleton, then $\varphi(x, y)$ is differentiable at x_0, y_0 and

$$\begin{aligned} 0 &= \nabla \varphi(x_0, y_0) \\ &= \left(\frac{\partial F}{\partial x}(x_0, y_0, m), \frac{\partial F}{\partial y}(x, y, m) \right). \end{aligned}$$

It suffices to look at the partial in x,

$$0 = -4m \frac{m - x}{(m + x)^3} \left(\frac{m - y}{m + y} \right)^2 e^{-2Lm},$$

to conclude that either $m = x$ or $m = y$. In either case, $\varphi(x, y) = F(x, y, m) = 0$, which is absurd. □

In the one-sided case, this result was sufficient because the only remaining possibility was to have two points equioscillating. However, in the two-sided case, we can equioscillate two or three points, but lemma 4.10 only says that there are at least two points equioscillating. Using the fact that $\varphi(x, y)$ has one-sided derivatives everywhere, and that for any direction γ this one-sided derivative $D_\gamma \varphi(x, y)$ must be non-negative at (x, y) we can obtain equioscillation of three points. First we must describe the shape of $F(x, y, m)$ as a function of m.

Lemma 4.11. *Let $1 \leq x \leq y$ (without loss of generality). The two local maxima $m_1(x,y) \leq m_2(x,y)$ of $F(x,y,m)$ inside $m > 1$ are given by*

$$\begin{aligned} m_1^2(x,y) &= \frac{2x+2y+Lx^2+Ly^2-\sqrt{p_{x,y}(L)}}{2L}, \\ m_2^2(x,y) &= \frac{2x+2y+Lx^2+Ly^2+\sqrt{p_{x,y}(L)}}{2L}, \\ p_{x,y}(L) &= (x^2-y^2)^2L^2+4(x^3-xy^2-x^2y+y^3)L \\ &\quad +4(x+y)^2 > 0. \end{aligned}$$

Furthermore, if $x < y$ then $m_1(x,y) \in (x,y)$ and $m_2 \in (y,\infty)$. If $x = y$, then $m_1(x,x) = x$ and $m_2(x,x) \in (x,\infty)$.

The critical points m_1 and m_2 also depend on L. When that dependence must be made explicit, we write $m_1(x,y,L)$ and $m_2(x,y,L)$.

Proof. We set the derivative $\partial F/\partial m$ to zero, obtaining

$$\begin{aligned} 0 &= \frac{\partial F}{\partial m}(x,y,m) \\ &= 2\frac{x-m}{(x+m)^3}\frac{y-m}{(y+m)^3}q_{x,y}(m)e^{-2Lm}, \\ q_{x,y}(m) &= -Lm^4+(2x+2y+Lx^2+Ly^2)m^2 \\ &\quad -(2y^2x-2x^2y-Lx^2y^2). \end{aligned}$$

The choices $m = x$ and $m = y$ lead to $F(x,y,m) = 0$ so they are minima, so we restrict our attention to $q_{x,y}(m) = 0$. By substituting $m^2 = n$ we obtain a quadratic polynomial in n whose roots are $m_1^2(x,y)$ and $m_2^2(x,y)$; we need to show that $1 \leq m_1 \leq m_2$. First to show that they are real, we show that the discriminant $p_{x,y}(L)$ is non-negative. It suffices to show that, as a quadratic polynomial over L, its coefficients are non-negative. The coefficient of L^2 and the constant coefficient are squares and hence non-negative. We rewrite $x = \lambda y$ with $\lambda \in (0,1]$ and substitute into the coefficient of L in $p_{x,y}(L)$ to obtain the expression $y^3(4\lambda^3-4\lambda^2-4\lambda+4) > 0$ since $y > 0$. Hence $p_{x,y}(L) > 0$ and $m_1 < m_2$.

Assume that $x < y$ are fixed. Since $F(x,y,x) = 0$ and $F(x,y,y) = 0$ but $F(x,y,m) > 0$ for any $m \in (x,y)$, there is a local maximum in m in the interval (x,y). Moreover, since $F(x,y,y) = 0$ and $\lim_{m\to\infty} F(x,y,m) = 0$, there must be another local maximum in the interval (y,∞). However, we have already shown that the only candidates for local maxima are m_1 and m_2, and since $m_1 \leq m_2$ it must be that $m_1 \in (x,y)$ and $m_2 \in (y,\infty)$. □

Lemma 4.12. *Let (x_0,y_0) minimize $\varphi(x,y)$. Then $M(x,y) = \{1, m_1(x,y), m_2(x,y)\}$ with $x \neq y$.*

Proof. The derivative of φ in the direction $\gamma = (\alpha,\beta)$ is given by

$$\begin{aligned} D_\gamma\varphi(x,y) &= \max_{m\in M(x,y)} \alpha\frac{\partial F}{\partial x}(x,y)+\beta\frac{\partial F}{\partial y}(x,y) \\ &= \max_{m\in M(x,y)} (\alpha,\beta)\cdot G(m), \end{aligned}$$

where

$$G(m) = 4me^{-2Lm}\frac{x-m}{(x+m)^2}\frac{y-m}{(y+m)^2}\left(\frac{y-m}{x+m},\frac{x-m}{y+m}\right).$$

In the case $x = y$, m_1 is actually a minimum so $M(x,x) = \{1, m_2(x,x)\}$ and in particular $x > 1$. The vectors

$$\left(\frac{x-1}{x+1},\frac{x-1}{x+1}\right) \quad \text{and} \quad \left(\frac{x-m_2}{x+m_2},\frac{x-m_2}{x+m_2}\right)$$

are parallel and of opposite directions, so it is not possible to choose a γ which will make the derivative negative. However, in the direction $(1,-1)$ the derivative is zero; we will now look at second order information. We set $g_m(\epsilon) = F(x+\epsilon, x-\epsilon, m)$, then

$$\begin{aligned} g_m'(0) &= 0, \\ g_m''(0) &= -16xme^{-2Lm}\frac{(m^2-x^2)^2}{(x+m)^8} < 0, \end{aligned}$$

for all $m \geq 1$, $m \neq x$ so for a sufficiently small ϵ, $\varphi(x+\epsilon, x-\epsilon) < \varphi(x,x)$, so it is not possible that $x_0 = y_0$.

Now we show that $G(m)$ and $G(n)$ are linearly independent for any $m, n \notin \{x, y\}$, so long as $x \neq y$. If not,

$$\begin{aligned} 0 &= \det \begin{pmatrix} \frac{y-m}{x+m} & \frac{x-m}{y+m} \\ \frac{y-n}{x+n} & \frac{x-n}{y+n} \end{pmatrix} \\ &= \frac{y-m}{x+m}\frac{x-n}{y+n} - \frac{x-m}{y+m}\frac{y-n}{x+n} \\ 0 &= (y^2-m^2)(x^2-n^2) - (x^2-m^2)(y^2-n^2) \\ \frac{y^2-n^2}{y^2-m^2} &= \frac{x^2-n^2}{x^2-m^2} \\ h(y^2) &= h(x^2), \end{aligned}$$

where $h(z) = (z-n^2)/(z-m^2)$. However, as a function of $[1,\infty)$, h is injective so $x^2 = y^2$, but since both are positive, we get that $x = y$, which we have assumed not to be the case. Hence $G(n)$ and $G(m)$ are linearly independent. In particular, there is a γ such that $\gamma \cdot G(n) < 0$ and $\gamma \cdot G(m) < 0$.

So if $M(x_0, y_0) = \{n, m\}$ (i.e., the set where the maximum is attained contains exactly two points $\{n, m\}$, which are either $\{1, m_1\}$, $\{1, m_2\}$ or $\{m_1, m_2\}$) then we have constructed a direction γ in which the one-sided derivative $D_\gamma \varphi^{(2)}(x_0, y_0)$ is negative, contradicting that $\varphi^{(1)}(x_0, y_0)$ is minimal. Therefore $M = \{1, m_1, m_2\}$, as required. □

We have shown that a minimum (x_0, y_0) gives three equioscillation points; we have to show that there is a unique choice of (x_0, y_0) giving three equioscillation points.

Lemma 4.13. *The system*

$$\begin{aligned} F(x,y,1) &= F(x,y,m_1(x,y)) \\ F(x,y,1) &= F(x,y,m_2(x,y)) \end{aligned}$$

has exactly two solutions (x_0, y_0) and (y_0, x_0) in $(1,\infty)^2$ with $x_0 \neq y_0$. This (x_0, y_0) is the unique (up to permutation (y_0, x_0)) minimizer of $\varphi(x, y)$. Moreover, x and y both increase monotonically as L decreases to 0.

$\alpha > -5/4$.

Proof. Without loss of generality, $x < y$. If we fix x and vary y then

$$\begin{aligned} \left(F(x,y,m_i)\right)_y &= F_y(x,y,m_i) + F_m(x,y,m_i)m_{i,y} \\ &= F_y(c,d,m_i) \\ &= -4m_i\frac{m_i-y}{(m_i+y)^3}\frac{(m_i-x)^2}{(m_i+x)^2}e^{-2Lm_i} \\ &= \frac{4m_i}{y^2-m_i^2}F(x,y,m_i), \end{aligned}$$

for $i = 0, 1, 2$ with $m_0 = 1$. Likewise,

$$\left(F(x,y,m_i)\right)_x = -4m_i\frac{m_i-x}{(m_i+x)^3}\frac{(m_i-y)^2}{(m_i+y)^2}e^{-2Lm_i} < 0.$$

Hence, $F(x,y,m_1)$ increases monotonically with y and decreases monotonically with x. Since $F(x,y,1)$ increases monotonically with x and y, there must be a unique $x = x(y) = x(y,L) \in (1,y)$ such that $F(x,y,1) = F(x,y,m_1(x,y))$. Now fix y_1 and $x_1 = x(y_1)$, then

$$\begin{aligned}\left.\frac{(F(x_1,y,m_1(x_1,y)))'}{(F(x_1,y,1))'}\right|_{y=y_1} &= \frac{\frac{4m_1}{y_1^2-m_1^2}F(x_1,y_1,m_1)}{\frac{4}{y_1^2-1}F(x_1,y_1,1)} \\ &= \frac{m_1(y_1^2-1)}{y_1^2-m_1^2} \\ &> \frac{y_1^2-m_1}{y_1^2-m_1^2} > \frac{y_1^2-m_1^2}{y_1^2-m_1^2} = 1\end{aligned}$$

Hence, $F(x_1,y,m_1(x_1,y))$ grows faster than $F(x_1,y,1)$ near $y = y_1$ and so if $y_2 - y_1 > 0$ is small, then it must be that $x(y_2) > x(y_1)$ and $x(y)$ is a strictly increasing function (in fact, $x'(y) > 0$).

Hence, $(F(x(y),y,m_2(x(y),y))' \le 0$ and $(F(x(y),y,1))' > 0$ and so there is a unique $y = y(L)$ giving $F(x(y),y,m_2(x(y),d)) = F(x(y),y,1)$.

Now let $\psi = F_L(x,y,m_1) - F_L(x,y,1)$ and $\eta = F_L(x,y,m_2) - F_L(x,y,m_1)$ and let us denote A, B the derivatives

$$\begin{aligned}A &= \begin{bmatrix} \psi_x & \psi_y \\ \eta_x & \eta_y \end{bmatrix} \text{ and} \\ B &= \begin{bmatrix} \psi_L \\ \eta_L \end{bmatrix},\end{aligned}$$

so that $(x_0'(L), y_0'(L)) = -A^{-1}B$. Direct calculations give that $A^{-1} = \alpha J$ where $\alpha > 0$ and

$$\begin{aligned}J &= \begin{bmatrix} \frac{m_2}{y^2-m_2^2} - \frac{1}{y^2-1} & \frac{1}{y^2-1} - \frac{m_1}{y^2-m_1^2} \\ \frac{1}{x^2-1} - \frac{m_2}{x^2-m_2^2} & \frac{m_1}{x^2-m_1^2} - \frac{1}{x^2-1} \end{bmatrix} = \begin{bmatrix} - & - \\ + & - \end{bmatrix}, \\ B &= 2F(x,y,1)\begin{bmatrix} 1-m_1 \\ 1-m_2 \end{bmatrix} = \begin{bmatrix} - \\ - \end{bmatrix}.\end{aligned}$$

Hence, $x_0'(L) < 0$. For $y_0'(L)$ we obtain

$$y_0'(L) = -2\alpha F(x_0,y_0,1)\frac{(m_2-1)(m_1-1)(m_1-m_2)(m_2m_1+m_1x_0^2+m_2x_0^2+x_0^2)}{(x_0^2-m_2^2)(x_0^2-1)(m_1^2-x_0^2)} < 0.$$

□

As in Lemma 4.8, we can give asymptotic approximations of the optimized coefficients, as well as an asymptotic convergence factor.

Lemma 4.14. *The asymptotically optimized coefficients as $L \to 0^+$ are*

$$x_0(L) = \frac{1}{8}8^{\frac{4}{5}}L^{-\frac{1}{5}}, \tag{17}$$

$$y_0(L) = \frac{1}{2}8^{\frac{2}{5}}L^{-\frac{3}{5}}. \tag{18}$$

The asymptotic convergence factor every other step is

$$\sqrt{F(x_0,y_0,1)} = 1 - 2(8L)^{\frac{1}{5}} + O(L^{\frac{2}{5}}).$$

Furthermore, if $L > O(N^\alpha)$, with $\alpha > -\frac{5}{4}$, then $M(x_0,y_0) \subset [1,N]$, and the optimized coefficients are the same for the frequency domains $[1,\infty)$ and $[1,N]$.

If the overlap L is $O(N^\alpha)$ with $\alpha < -\frac{5}{4}$, then it may be possible to find better coefficients than the ones given (our analysis in Section 4.5 is such a case). However, the convergence factor estimate holds even in that case.

Proof. The motivation comes from writing x, y, L in terms of a new variable z. We let $x = 1/z$, $y = b/z^j$ and $L = az^k$, which we then substitute into $\psi = F(x, y, m_1(x, y)) - F(x, y, 1)$ and $\eta = F(x, y, m_2(x, y)) - F(x, y, 1)$. When $j = 3$ and $k = 5$, we find that we can approximate ψ and η linearly, to obtain

$$\begin{aligned} \psi &= \left(4 - \frac{8}{\sqrt{b}}\right) z + o(z), \\ \eta &= \left(4 - 4\sqrt{2ab}\right) y + o(y). \end{aligned}$$

We set the coefficient of of z in ψ to zero to obtain that $b = 4$. Substituting into η and setting the coefficient of z to zero, we obtain that $a = 1/8$. Finally, we express x_0 and y_0 in terms of L, obtaining equations (17), (18).

Substituting (17), (18) then $L = N^\alpha$ in m_2 and proceeding as with equation (16), we see that

$$\frac{m_2}{N} \quad \to \quad 0$$

when $\alpha > -5/4$ and diverges when $\alpha < -5/4$. □

Although we do not perform a semidiscrete analysis in the two parameter case that is as detailed as the one we performed in the single parameter case, the fact that $M(x_0, y_0) \subset [1, N]$ is still important because the discretization will certainly limit the highest frequency that can be observed. If $M(x_0, y_0)$ lies outside of $[1, N]$, it would be possible to improve the convergence factor over the frequencies $[1, N]$ by choosing different parameters (x_0, y_0). The constraint that $L > O(N^{-\frac{5}{4}})$ allows some anisotropy of the mesh while keeping the optimized coefficients close to those of the continuous system. For extremely small values of L relative to $1/N$ (i.e., $\alpha < -5/4$), it may be possible to improve upon the optimized coefficients given in this paper.

This completes the proof of the second part of Theorem 2.1.

4.4 OO2 one-sided analysis, $L > 0$.

For the second order operators, the optimization problem is

$$\begin{aligned} G(s, t, m) &= G_L(s, t, m) = \left(\frac{s + tm^2 - m}{s + tm^2 + m}\right)^2 e^{-Lm}, \\ \varphi(s, t) &= \max_{m \in [1, \infty]} G(s, t, m). \end{aligned} \tag{19}$$

The convergence factor every other step, for a given choice of s, t, is $\varphi(s, t)$.

Lemma 4.15. *For any given $L > 0$, there is a unique (s_0, t_0) minimizing $\varphi(s, t)$. Furthermore, if $L = L(N) > O(N^\alpha)$, $\alpha > -5/4$ then for all sufficiently large N, (s_0, t_0) also minimizes $G(s_0, t_0, m)$ over m ranging in $[1, N]$. The optimized parameters are the unique solution of*

$$\begin{aligned} G(s, t, 1) &= G(s, t, m_1(x, y)) \\ G(s, t, 1) &= G(s, t, m_2(x, y)), \end{aligned}$$

where $x = \frac{1 - \sqrt{1 - 4st}}{2t}$ and $y = \frac{1 + \sqrt{1 - 4st}}{2t}$. We use the asymptotic formulae

$$s_0 = \frac{1}{2} 2^{\frac{3}{5}} L^{-\frac{1}{5}}, \tag{20}$$

$$t_0 = \frac{1}{2} 2^{\frac{1}{5}} L^{\frac{3}{5}}; \tag{21}$$

leading to the asymptotic convergence factor every other step of

$$G(s_0, t_0, 1) = 1 - 2 \cdot 2^{\frac{2}{5}} L^{\frac{1}{5}} + O(L^{\frac{2}{5}}). \tag{22}$$

Proof. We may rewrite

$$G = \frac{x-m}{x+m}\frac{y-m}{y+m}e^{-Lm}.$$

Since the values x, y can be used to parametrize the problem (and s, t may be recovered from x, y), we may invoke lemma 4.13 to conclude that x, y are real and unique (up to permutation) and so s, t are real and unique.

Next, we replace (17) and (18) into $x = \frac{1-\sqrt{1-4st}}{2t}$ and $y = \frac{1+\sqrt{1-4st}}{2t}$. A series expansion leads to equations (20) and (21). We substitute these parameters into $G(s_0, t_0, 1)$ and expand into a series to obtain the asymptotic convergence factor (22). □

This completes the proof of Theorem 2.2.

4.5 The $L = 0$ case.

For the zeroth order, one-sided case, the envelope theorem still asserts that there has to be equioscillation. Since $\lim_{m\to\infty} F(x, m) = 1$, we must concentrate on the $[1, N]$ case. By inspection, the maxima are at 1 and N and the value of the optimal parameter $\tilde{x}$ is given by solving $F(x, 1) = F(x, N)$, which has the unique solution

$$\tilde{x} = \sqrt{N}.$$

Substituting into $F(x, 1)$ we obtain

$$\varphi(\tilde{x}) = \frac{(\sqrt{N}-1)^2}{(\sqrt{N}+1)^2} \approx 1 - 4N^{-\frac{1}{2}}$$

as $N \to \infty$. By comparison, the convergence factor estimate of Theorem 2.1 with an overlap $L \approx 1/N$ (approximately one grid length of overlap) gives a convergence factor of approximately $1 - 4N^{-\frac{1}{3}}$. Hence, to obtain a solution with a given tolerance, the zero overlap algorithm must iterate $O(N^{\frac{1}{2}})$ times, while the algorithm with one grid length of overlap must iterate $O(N^{\frac{1}{3}})$ times.

For the two-sided zeroth order case, the Envelope Theorem gives an equioscillation of two points. The only interior maximum in $m > 0$ is

$$m(x, y) = \sqrt{xy}.$$

The only possibility to obtain three equioscillation points is if

$$F(x, y, 1) = F(x, y, m(x, y)) = F(x, y, N), \tag{23}$$

and the proof of Lemma 4.13 shows that if there are only two equioscillation points, then there is a direction of the (x, y) plane such that these two equioscillating points are simultaneously decreasing. Therefore the unique minimizer is the unique solution (up to permutation) of equation (23) in the domain $[1, N] \times [1, N]$, given by

$$x = \sqrt{2}\frac{N^{\frac{3}{4}}}{\sqrt{N+1}+\sqrt{N}-1}, \tag{24}$$

$$y = \frac{\sqrt{2}}{2}N^{\frac{1}{4}}(\sqrt{N+1}+N^{\frac{1}{2}}-1), \tag{25}$$

$$\varphi(x, y) = 1 - 4\sqrt{2}N^{-\frac{1}{4}} + O(N^{-\frac{1}{2}}).$$

We see again that the algorithm with zero overlap converges within a given tolerance in $O(N^{\frac{1}{4}})$ steps, while the algorithm with one grid length of overlap converges in $O(N^{\frac{1}{5}})$ steps.

A similar argument applies to the one-sided estimate for the second order tangential transmission conditions. We summarize this choice of parameters.

Lemma 4.16. *(Optimized transmission conditions, zero overlap.) Let $a = b$, and consider only the frequency spectrum $[1, N]$ (there are $2N+1$ grid points on the interface). The one-sided optimized Robin parameter is $c = \sec a\sqrt{N}$, yielding a convergence factor every other step of*

$$\frac{(\sqrt{N}-1)^2}{(\sqrt{N}+1)^2} = 1 - 4N^{-\frac{1}{2}} + O(N^{-1}).$$

The two-sided optimized Robin parameters are

$$\begin{aligned} c &= x \sec a, \\ d &= y \sec a; \end{aligned}$$

where x and y are given by (24) and (25). The convergence factor is $1 - 2\sqrt{2}N^{-\frac{1}{4}} + O(N^{-\frac{1}{2}})$. The one-sided optimized second order tangential parameters are

$$\begin{aligned} c &= s \sec a, \\ d &= t \sec a; \end{aligned}$$

where $x = \frac{1-\sqrt{1-4st}}{2t}$ and $y = \frac{1+\sqrt{1-4st}}{2t}$ and x, y are given by (24) and (25).

In practice, the second order tangential operator $\partial^2/\partial\theta^2$ will be approximated discretely, so we have attempted to replace it by the finite difference approximation

$$\Lambda u = \frac{\partial^2}{\partial\theta^2} u \quad \approx \quad \frac{u_{k+1} + u_{k-1} - 2u_k}{h^2} = \Lambda_h u.$$

The Fourier transform of Λ is $\hat{\Lambda}(m) = -m^2$, which leads to our analysis but the Fourier transform of Λ_h is $\hat{\Lambda}_h(m) = \frac{2\cos mh - 2}{h^2}$. So F is replaced by

$$F_h(c, d, m) \quad = \quad \frac{(c + 2d\frac{\cos mh - 1}{h^2} - m)^2}{(c + 2d\frac{\cos mh - 1}{h^2} + m)^2} e^{-2Lm}.$$

The periodicity of the cosine function means that $m \mapsto F_h(c, d, m)$ has infinitely many local maxima $m_{1,h}(c, d), m_{2,h}(c, d), \ldots$ We simplify the problem by considering only the nonoverlapping case (with $L = 0$). Because h is small, when m is small, we have that $\cos mh \approx 1 - (mh)^2/2$, which is to say, $F_h(c, d, 1) \approx F(c, d, 1)$. If we equioscillate $F(c, d, 1) = F_h(c, d, m_{1,h}) = F_h(c, d, m_{2,h})$, we see that $m_{j,h} > N$ for $j = 3, 4, \ldots$ and we obtain the following result.

Proposition 4.17. *(Second order tangential transmission operator, semidiscrete, nonoverlapping.) The semidiscrete analysis leads to slightly different parameters c' and d' given by*

$$\begin{aligned} \alpha &= \frac{N\pi^4 + 8N^3\pi^2 - N^2(8\pi^2 + \pi^4) + N\pi^4}{4\pi^4 - 64\pi^2N^2 + 256N^4}, \\ \tilde{c} &= \frac{N(8n - \pi^2)}{2\alpha^{\frac{1}{4}}(8N^2 - \pi^2)}, \\ \tilde{d} &= \frac{2\alpha^{\frac{3}{4}}(8N^2 - \pi^2)}{N(8N - \pi^2)}. \end{aligned}$$

The convergence factor is almost identical to the analysis of Lemma 4.16.

5 Numerical simulations

For our numerical simulations, we have two implementations. One is a semispectral discretization, which is one of the most widely used discretizations in meteorology. The second is a finite element discretization.

As has already been mentioned, the various iterations converge modulo the constant mode. This makes error estimation more complicated. In the semispectral code, we compute the error by taking the trace of the function along the interface, subtracting the mean, and computing the L^2 norm of the result. In the finite element code, we use instead the seminorm $\int_{\Omega_1} \nabla u \cdot \nabla u$, which is not equivalent to using the L^2 norm of the trace, but which may be more natural in a finite element code. In view of Gelfand's spectral radius formula, the asymptotic convergence factor should be the same regardless of which vector norm is used to measure the errors.

5.1 The semispectral code

The semispectral discretization uses a latlong grid, i.e., a uniform grid in (φ, θ). The Fourier coefficients $\hat{u}(\phi, k)$ are computed using the Fast Fourier Transform, and the system (3) is discretized in φ using a centered finite difference. The boundary conditions for each ODE are given by (4) and (5), for solving over the entire sphere Ω. For solving on a subdomain whose boundaries are latitudes, one or both of these boundary conditions are replaced by the Dirichlet, Robin (OO0) or second order tangential (OO2) transmission operators. In all cases, we use initial solutions that are random, while the right hand side f is zero. We remark that a random right hand side f can be reduced to this situation.

5.1.1 Implementing the transmission conditions in the semispectral code

In the semispectral code, subdomains must be latitudinal, exactly as in our analysis and as per Figure 1. A boundary condition of the Robin type (e.g., $\psi u = cu$) leads to a boundary condition of the form

$$(c + \frac{\partial}{\partial \phi})\hat{u}_{k+1}(a, m) = (c + \frac{\partial}{\partial \phi})\hat{v}_k.$$

Similarly, an OO2 condition of the form $\psi u = cu + du_{\theta\theta}$ leads to the transmission condition

$$((c + dm^2) + \frac{\partial}{\partial \phi})\hat{u}_{k+1}(a, m) = ((c + dm^2) + \frac{\partial}{\partial \phi})\hat{v}_k.$$

The optimal, nonlocal operator given by $\hat{\psi}(m) = |m|/\sin a$ is implemented using the transmission condition

$$(|m|/\sin a + \frac{\partial}{\partial \phi})\hat{u}_{k+1}(a, m) = (|m|/\sin a + \frac{\partial}{\partial \phi})\hat{v}_k.$$

We make similar considerations for $\hat{v}_{k+1}$ and $\hat{u}_k$.

Our semispectral solver is implemented using Fast Fourier Transforms, which gives very good performance. In this case, implementing any of the transmission conditions is equally easy, so it is natural to use the optimal transmission conditions based on the nonlocal operator.

5.1.2 Results

Numerical results for the semispectral codes are summarized in Figure 2. We chose the various tolerances so that all the convergence curves are visible, distinct, and show clearly how the convergence behavior changes over the first few iterations. The semispectral solver is limited to domain decompositions where the subdomains have latitudinal boundaries, as per Figure 1. Our finite element code, in the next section, can use domain decompositions with arbitrary subdomains. In all of our grids, we use $2N + 1$ grid points in the θ variable, and $N + 2$ grid points in the φ variable. All of these grids use $N = 50$, and the θ grid is given by $\theta = 0,\ 2\pi/102,\ \ldots\ ,\ 202\pi/102$ and the grid in φ is given by $\varphi = 0,\ \pi/51,\ \ldots\ , \pi$. When specifying the right-hand-side f, it is necessary to ensure that $f(0, \theta)$ and $f(\pi, \theta)$ are constant functions of θ.

In Figure 2 (a), we have computed iterates of the Schwarz iterations until the L^2 error on colatitude $a = b = \pi/2$ (the equator) is less than 10^{-6} and plotted the error at each even iteration to match with the analysis in the text. The error is measured modulo the constant mode. Since there is no overlap, the classical Schwarz iteration does not converge and we have not plotted it. The transmission operators are Robin (OO0), second order tangential with coefficients (c, d) (OO2), and the slightly improved semidiscrete coefficients coefficients (c', d') (OO2') and a discretized optimal and nonlocal operator. The OO0 iteration converges in 88 iterations, while the OO2 and OO2' iterations converge in 16 iterations, and the nonlocal operator leads to convergence in 12 iterations. This grid has $N = 50$, or 101 grid points in θ and 52 grid points in φ.

In Figure 2 (b), we have plotted the convergence of the various Schwarz algorithms with six latitudinal subdomains and without overlap.

In (c) and (d), we have similar graphs in the case of overlap. In (c), we have two subdomains, and an overlap between these two subdomains which measures $\Delta\varphi = 2\pi/(N + 1) = 2\pi/31$. The Dirichlet (classical) Schwarz method converges to tolerance 10^{-6} in 140 iterations, the OO0 method converges in 36 iterations, the OO2 method converges in 14 iterations, and the nonlocal operator converges in 4 iterations.

In (d), we have six subdomains and an overlap between each pair of adjacent subdomains of $\Delta\varphi = \pi/31$.

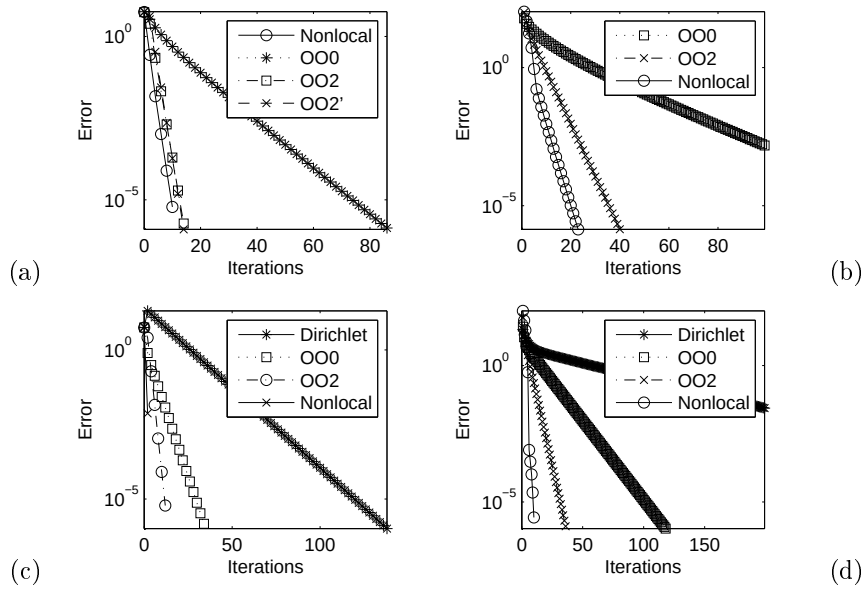

Figure 2: Numerical results, semispectral code. (a): convergence with two latitudinal subdomains and zero overlap. (b): convergence with six latitudinal subdomains and zero overlap. (c): convergence with two latitudinal subdomains and two grid lengths of overlap. (d): convergence with six latitudinal subdomains, the overlaps are each the length of one grid interval.

N	Dirichlet	OO0	OO2	Optimal
8	20	8	4	2
16	40	14	6	2
32	84	26	10	2
64	172	42	14	2
128	360	58	18	2
256	768	104	22	2

Table 1: Iteration counts as we vary $L = \pi/(N+2)$.

5.1.3 Scaling in h the semispectral code, 2 subdomains, minimal overlap $L = h$

In this set of experiments, we have computed the iteration count, as well as an approximation of the convergence factor, as we vary N and with $L = \pi/(N+2)$. The iteration counts are given in Table 1. The grid parameter h varies nonuniformly across the sphere, but near the equator, we have that $h \approx L = \pi/(N+1)$. We also approximate the convergence factor as follows. At each iteration k, we compute the norm of the error e_k, as we did in the previous section. We then approximate the convergence factor using $\rho \approx (e_n - e_m)^{1/|n-m|}$. We iterate until the error e_n is less than 10^{-6}, and we let $m = \lfloor n/2 \rfloor$. The convergence factors are plotted in Figure 3. The convergence factor for the classical Schwarz method, marked Dirichlet, is a good fit for the $1 - O(h)$ convergence rate, in the sense that it seems to approach 1 almost linearly. We can also see the convergence factor $1 - O(h^{1/3})$ for the OO0 method, although a smaller value of h would illustrate more clearly the power 1/3 in the convergence factor.

The OO2 method is extremely fast, with a very small convergence factor. Our theory predicts a convergence factor of $1 - O(h^{1/5})$. Therefore, in order to have a convergence factor which is larger than 0.9, we would require $h \approx 10^{-5}$, which is to say, $N \approx 10^5$. Such a grid would contain approximately 10^{10} points. Aside from possible numerical difficulties with the double precision representation, such a large grid is not possible on the laptop computer used to produce these experiments. On the one hand, this means that it is difficult to numerically probe the asymptotic behavior of the OO2 method. On the other hand, this also means that the OO2 method should be good enough for most current applications.

The Optimal method has a very small convergence factor, of the order 10^{-4}, and it does not appear to

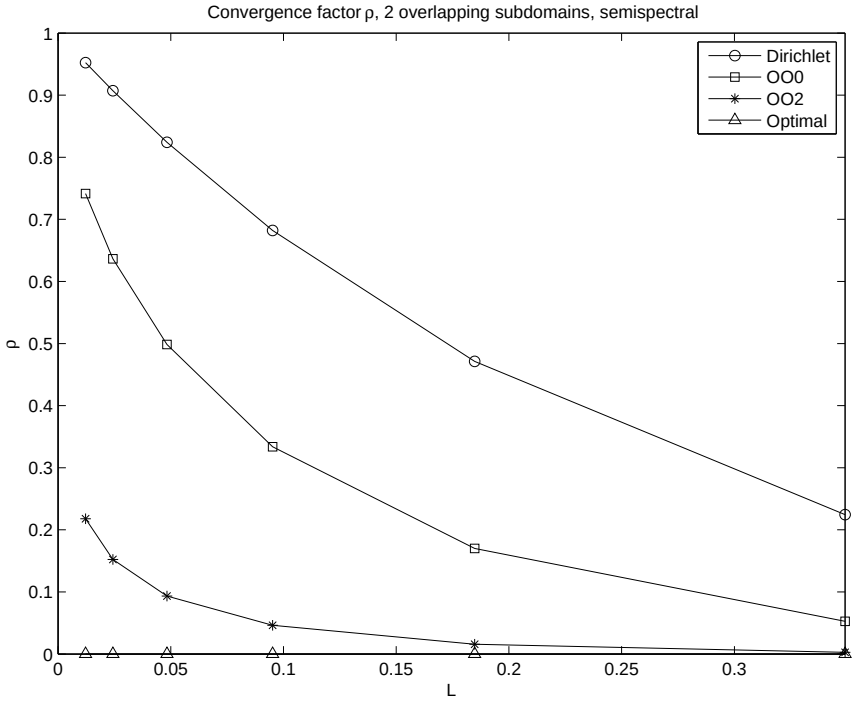

Figure 3: Convergence factor as we vary $h = L = \pi/(N+2)$, semispectral code, two subdomains.

vary with N.

5.2 Scaling in h the semispectral code, 2 subdomains, thick overlap $L = h$

In this section, we perform an experiment similar to the one of Section 5.1.3, but we now keep a constant geometric overlap size of $pi/10$ radians (i.e, $a - b = \pi/10$). As can be observed in Figure 4, the convergence factor does not appear to vary with h.

5.3 Scaling in h the semispectral code, 2 subdomains, nonoverlapping

We perform an experiment similar to the one of Section 5.1.3, but with zero overlap. The convergence factor does not appear to vary with h.

5.4 Finite element solver

For our finite element solver, we rephrase the Laplace problem in the variational form

$$\text{Find } u \in H^1(\Omega) \text{ such that } \int_\Omega \nabla u \cdot \nabla v = \int_\Omega fv, \text{ for all } v \in H^1(\Omega).$$

A simple way to understand the gradients appearing in the variational formulation is as follows. Let u be a function defined on the sphere $\Omega \subset \mathbb{R}^3$. We can extend u to all of $\mathbb{R}^3$ by putting

$$u(\mathbf{x}) = u(\mathbf{x}/\|\mathbf{x}\|). \tag{26}$$

Then we can use the usual definition of the gradient, $\nabla u = (u_x, u_y, u_z)$. According to the discussion in Section 3, we must now choose a suitable finite element basis of functions that are constant on half-rays, i.e., such that $u(\mathbf{x}) = u(\lambda\mathbf{x})$ for every $\lambda > 0$ and every $\mathbf{x} \in \mathbb{R}^3$.

To define a finite element discretization, we must first build a mesh Ω_h for the sphere. Because we are integrating on the sphere, we build our mesh from *spherical triangles* $\{\nu_1, ..., \nu_n\} = \Omega_h$, triangles on the

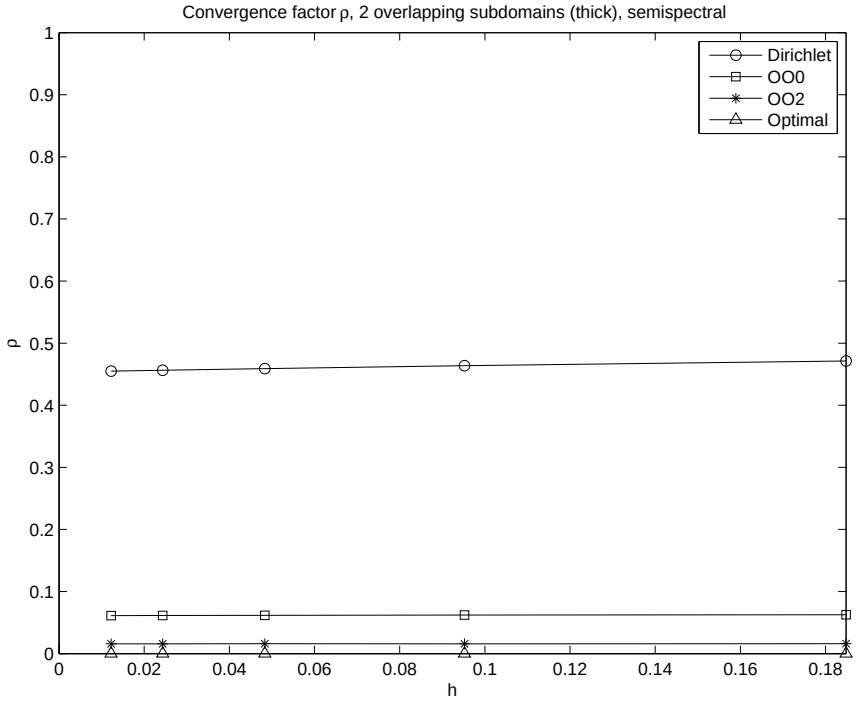

Figure 4: Convergence factor as we vary h, semispectral code, two subdomains, with $a - b = \pi/10$ constant across all values of h ("thick overlap").

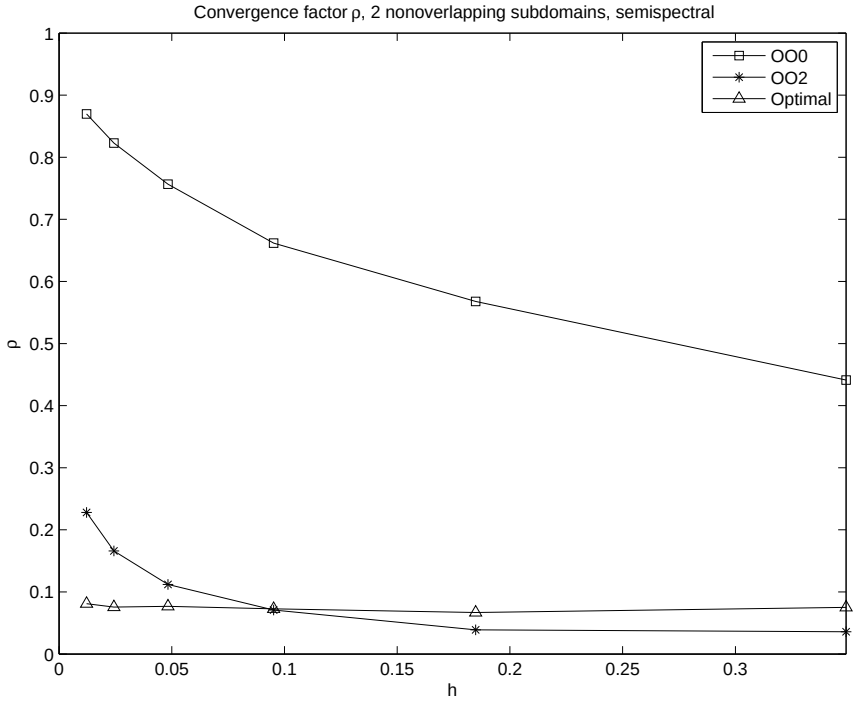

Figure 5: Convergence factor as we vary h, semispectral code, two subdomains, nonoverlapping.

sphere whose edges are great circles. Because our elements are curvilinear, it is not obvious how to define the basis functions. We can approximate the sphere Ω by a polyhedron $T_h = \{K_1, ..., K_n\}$, simply by replacing all spherical triangles in our mesh Ω_h with Euclidian triangles with the same vertices. On T_h, we could use $V_h(\Omega_h)$, the space of piecewise linear functions as a finite element space on Ω_h, but this does not immediately give rise to a finite element space on Ω and our mesh of curvilinear triangles.

We can prolong the basis functions on our polyhedral approximation Ω_h of Ω, to basis functions on all of $\mathbb{R}^3$. If φ is a piecewise linear function on T_h, we prolong it to all of $\mathbb{R}^3$ by saying that, for every triangle $K = \{\mathbf{x}_1, \mathbf{x}_2, \mathbf{x}_3\} \in T_h$, and for every $\mathbf{x} \in K$, and for every $\lambda > 0$, $\varphi(\lambda \mathbf{x}) = \lambda \varphi(\mathbf{x})$; in other words, $\varphi(x, y, z) = ax + by + cz$ on the "cone" $\mathbb{R}^+ K$. The set $V_h(\mathbb{R}^3)$ obtained in this way has two problems. First, these functions are not radially constant (which we require). Second, $V_h(\mathbb{R}^3)$ does not contain any constant functions (except for $\varphi = 0$), even though $V_h(\Omega_h)$ does contain the constant functions. Hence, once we restrict to the sphere Ω, the space $V_h(\mathbb{R}^3)|_\Omega$ also does not contain the constants. The constants are very important because they are precisely the kernel of the spherical Laplacian.[1]

We choose a finite element space V_h on Ω which contains the constants, and whose functions are all radially constant. One may then check that the Schwarz algorithms act on the constants and on the orthogonal complement of the constants in independent ways, and so our analysis holds and the algorithms converge. Let $K \in T_h$ be a triangle and (p, q, r) be its outward pointing normal. One way to obtain such a space is to take our linear function $\varphi(x, y, z) = ax + by + cz$ on K and to define $\tilde{\varphi}(x, y, z) = \varphi(s \cdot (x, y, z))$ where $s = \frac{(p,q,r) \cdot \mathbf{x}_1}{px + qy + rz} \in \mathbb{R}$, and hence $s \cdot (x, y, z)$ is contained in the Euclidian triangle K. Our resulting basis functions are *piecewise rational linear*, and

$$\tilde{\varphi}(x, y, z) = C \frac{ax + by + cz}{px + qy + rz} \text{ for all } (x, y, z) \in (0, \infty) \cdot K;$$

for some real constant C. One could build higher order finite element basis functions by using linear combinations of rational functions p/q where p and q are homogeneous polynomials of the same degree. Although our derivation is not the same, the resulting finite elements coincide with the ones analyzed in [1]. Other possible finite elements include continuous elements based on spherical coordinates [30], and discontinuous elements [6], [11]. These alternate finite element spaces have not been analyzed in this paper.

Our finite elements are piecewise rational linear. Because quotients of homogeneous linear polynomials are constant along half-rays through the origin, equation (26) is automatically satisfied.

On each subdomain, we solve a Robin or second order tangential boundary value problem. We denote by D_ν the directional derivative in the direction of the unit outward pointing normal ν of a given subdomain Ω_i (note that ν tangent to Ω). Similarly, we denote by D_τ the directional derivative in the direction tangential to the boundary of Ω_i. The direction of the tangent is chosen once and for all and does not matter, since we are interested in the second tangential derivative D_τ^2. The relationship between these "geometric" derivatives and the derivatives D_θ and D_φ for latitudinal subdomains are given by $D_\varphi = \pm D_\nu$ and $D_\theta = r D_\tau$, where $r = \sin\varphi$ is the radius of the latitude φ. On each subdomain Ω_i, at iteration k, we are solving the partial differential equation $-\Delta u_k^{(i)} = f$ with boundary condition $\alpha u_k^{(i)} - \beta D_\tau^2 u_k^{(i)} + D_\nu u_k^{(i)} = \alpha v_k - \beta D_\tau^2 v_k + D_\nu v_k$. In this problem, f and v_k are the data, and $u_k^{(i)}$ is the unknown. The variational formulation of this problem is

$$\begin{aligned}
&\text{Find } u = u_k^{(i)} \in H^1(\Omega_i) \text{ such that, for all } w \in H^1(\Omega_i), \\
&\int_{\Omega_i} \nabla u \cdot \nabla w + \alpha \int_{\partial\Omega_i} uw + \beta \int_{\partial\Omega_i} (D_\tau u)(D_\tau w) \\
&= \int_\Omega fw - \int_{\Omega \setminus \Omega_i} \nabla v_k \cdot \nabla w + \alpha \int_{\partial\Omega_i} v_k w + \beta \int_{\partial\Omega_i} (D_\tau v_k)(D_\tau w).
\end{aligned}$$

The "reconstituted iterate" v_k is given by $v_k = \omega_1 u_{k-1}^{(1)} + ... + \omega_p u_{k-1}^{(p)}$, where $u_{k-1}^{(i)}$, $i = 1, ..., p$ is the solution on subdomain Ω_i (and there are p subdomains). The functions $\omega_1, ..., \omega_p$ form a partition of unity.

For the Robin condition (i.e., $\beta = 0$), we use the one-sided optimized parameter $\alpha = e^{-\frac{1}{3}} r^{-1}$. Here, e is an estimate of the thickness of the overlap (we measure the Euclidian distance between the two interfaces) and $r = \sin\varphi$ is the radius of the latitudinal boundary (if the boundary is latitudinal), and when the boundary

[1] It is tempting to generate basis functions by setting $\tilde{\varphi}(\mathbf{x}) = \varphi(\mathbf{x}/|\mathbf{x}|)$, cf. (26). However, this finite element space does not contain the constant functions either.

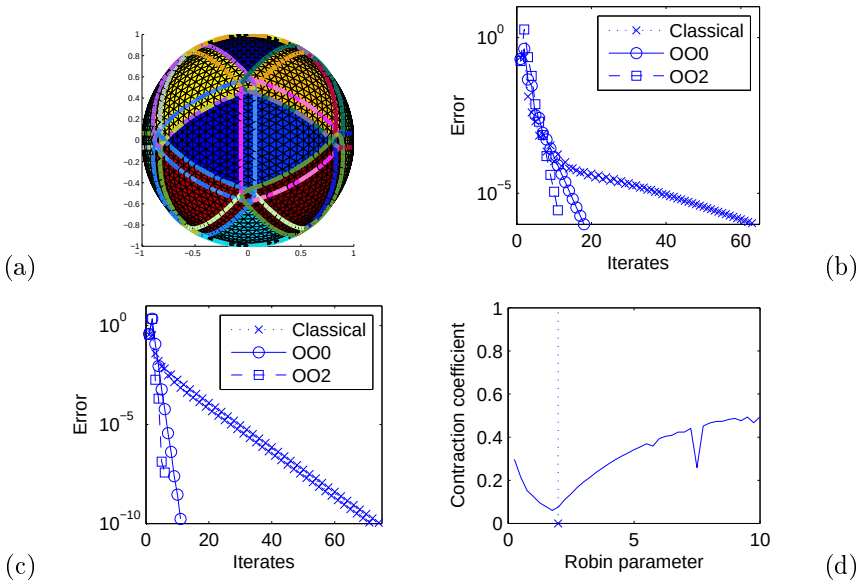

Figure 6: (a): An icosahedral grid with 20 subdomains. (b): Convergence of classical and optimized Schwarz methods for the grid of (a). (c): Convergence of classical and optimized Schwarz methods, for two nearly hemispherical overlapping subdomains, (d): The accuracy of the optimized Schwarz coefficient chosen in (c).

is not latitudinal, we use the heuristic $r := |\partial\Omega_i|/(2\pi)$. The length $|\partial\Omega_i|$ of the boundary of Ω_i can be computed from the bilinear form of $\int_{\partial\Omega_i} uw$, which is available because we are solving a Robin problem, by substituting $u = 1$ and $w = 1$.

For the second order tangential boundary condition, we use the one-sided optimized parameters $\alpha = 1/2 \cdot 2^{3/5} e^{-1/5}/r$ and $\beta = 1/2 \cdot 2^{1/5} e^{3/5} r^2$.

We did not implement the optimal (nonlocal) transmission operator for the finite element grid. One could in principle compute this operator, e.g., using a Schur complement, or by computing the matrix square root of a discretization of the second tangential derivative on the interface. We were not able to produce an algorithm of this type which had any performance advantage over an LU decomposition of the whole system. One could also use a regular grid and fast Fourier transforms; this was discussed in Section 5.1.1 on the semispectral implementation. When there are multiple subdomains that meet at corners, such as Figure 6 (a), such optimal or nilpotent transmission operators are not even known.

Although the analysis is based on our spherical triangle grid Ω_h, for visualisation purposes, we use the polyhedral approximation T_h. The triangulation T_h is obtain by using an icosahedron and subdividing the triangles (which is known as the icosahedral grid.)

In Figure 6 (a), we show an icosahedral grid with 2562 vertices. The finite element discretization of the Laplacian for that mesh is a 2562×2562 sparse matrix. We use this mesh, which does not correspond to our analysis, to show that our optimized transmission conditions work well even when the subdomains do not have latitudinal interfaces. In (b), we plot the convergence histories of the various Schwarz algorithms, for the mesh with 20 subdomains depicted in (a). To compute the error, we use the bilinear form of the Laplacian as a seminorm, i.e., the error on the kth step is $\int_\Omega \nabla(v_k - u) \cdot \nabla(v_k - u)$, where u is the converged solution. This seminorm is equivalent to the $H^1(\Omega)$ norm, modulo constant functions. In (b), we see that the classical Schwarz algorithm (dotted) converges but nearly stagnates, while the optimized Schwarz algorithms, given by the solid (Robin or OO0) and dashed (second order or OO2) lines converge very quickly. The classical Schwarz iteration converges to a tolerance of 10^{-6} in 65 iterations, while the OO0 iteration converges to the same tolerance in 19 iterations and the OO2 iteration converges in 12 iterations. In (c), we have a similar graph but with two nearly hemispherical subdomains, and an overlap of exactly two elements. This "hemihedral grid" is obtained as follows. First, we subdivide the icosahedron four times (the same number of subdivisions as in (a)). Second, we select triangles from this mesh to form two exactly hemispherical, disjoint subdomains. Finally, we add one row of elements to each hemispherical subdomain. The classical Schwarz iteration converges to an error less than 10^{-10} in 75 iterations. By comparison, the OO0 iteration

converges to the same tolerance in 12 iterations, and the OO2 converges to the same tolerance in 7 iterations. In (d), we have measured the convergence factor (or contraction coefficient ρ) of (c), by computing the ratio of the errors at iterations 6 and 10, and taking the fourth root, for various values of the Robin parameter α. The vertical dotted line is our optimized Robin coefficient, and we see that it lines up very well with the numerically observed optimal coefficient.

6 Conclusions

We have given optimal and optimized transmission operators for the Laplace problem on the sphere and have shown that they perform much better than the classical iteration with a Dirichlet condition. We have computed convergence factors for the one-sided and two-sided Robin condition and two choices of second-order tangential operators, and compared them against the discretized optimal nonlocal operator. A similar analysis for the positive definite Helmholtz problem will be detailed in a later paper.

Acknowledgements

The authors would like to thank the anonymous reviewers for their helpful comments.

References

[1] Baumgardner, J., Frederickson, O., Icosahedral Discretization of the Two-Sphere. SIAM J. Num. Anal., 22(6):1107–1115, 1985.

[2] Chevalier, P., Nataf, F., Symmetrized method with optimized second-order conditions for the Helmholtz equation. Contemp. Math., pages 400–407, 1998.

[3] Chniti, C., Nataf, F., Nier, F., Improved interface conditions for a non-overlapping domain decomposition of a non-convex polygonal domain. C. R. Math. Acad. Sci., 342(11):883–886, 2006.

[4] Côté, M. J. Gander, L. Laayouni, and S. Loisel, Comparison of the Dirichlet-Neumann and Optimal Schwarz Method on the Sphere. In R. Kornhuber, R. Hoppe, J. Priaux, O. Pironneau, O. B. Widlund, and J. Xu (editors), Domain Decomposition Methods in Science and Engineering, Lecture Notes in Computational Science and Engineering, vol. 40, Springer, 2004, pp.235-242.

[5] Côté, J. and Staniforth, A. An accurate and efficient finite-element global model of the shallow-water equations. Mon. Wea. Rev., 118 (1990), pp. 2707-2717.

[6] Demlow, A., Dziuk, G., An adaptive finite element method for the Laplace-Beltrami operator on implicitly defined surfaces. SIAM J. Numer. Anal., 45(1):421–442, 2007.

[7] Deng, Q., An optimal parallel nonoverlapping domain decomposition iterative procedure. SIAM J. Num. Anal., 41(3):964–982, 2003.

[8] V. Dolean, S. Lanteri, F. Nataf, Optimized Interface Conditions for Domain Decomposition Methods in Fluid Dynamics, Int. J. Numer. Meth. Fluids, 40, 1539-1550, 2002.

[9] Dubois, O., Optimized Schwarz methods for the advection-diffusion equation. Master's thesis, McGill University, 2003.

[10] Dubois, O., Gander., M., Loisel, S., St-Cyr, A., Szyld, D., The Optimized Schwarz Method with a Coarse Grid Correction (in preparation).

[11] Dziuk, G., Elliott., C., Finite elements on evolving surfaces. IMA J. Numer. Anal., 27(2):262–292, 2007.

[12] Flauraud, E., Nataf, F., Willien, F., Optimized interface conditions in domain decomposition methods for problems with extreme contrasts in the coefficients. J. Comput. Appl. Math., 189(1–2):539–554, 2006.

[13] Gander, M., Halpern, L., Nataf, F., Optimal convergence for overlapping and non-overlapping Schwarz waveform relaxation. In C.-H. Lai, P. E. Bjorstad, M. Cross, and O. Widlund (editors), 11th international conference on domain decomposition methods, ddm.org, 1999.

[14] Gander, M. J., Optimized Schwarz Methods. SIAM Journal on Numerical Analysis, Vol. 44, No. 2, pp. 699-731, 2006.

[15] Gander, M., Golub, G., A non-overlapping optimized Schwarz method which converges with arbitrarily weak dependence on h. In I. Herrera, D. Keyes, O. Widlund and R. Yates (editors), Proceedings of the 14th International Conference on Domain Decomposition, published by National Autonomous University of Mexico, pp. 281-288, 2003.

[16] Gander, M. J., Halpern, L., Absorbing boundary conditions for the wave equation and parallel computing. Math. of Comp., 74(249):153–176, 2004.

[17] Gander, M. J., Halpern, L., Optimized Schwarz Waveform Relaxation for Advection Reaction Diffusion Problems. SIAM Journal on Numerical Analysis, Vol. 45, No. 2, pp. 666-697, 2007.

[18] M.J. Gander, L. Halpern, C. Japhet, Optimized Schwarz Algorithms for Coupling Convection and Convection-Diffusion Problems. In N. Debit, M. Garbey, R. Hoppe, J. Périaux, D. Keyes, Y. Kuznetsov, editors, Proceedings of the Thirteenth International Conference on Domain Decomposition Methods, pages 253-260. ddm.org, 2001.

[19] Gander, M., Halpern, L., Nataf, F., Optimized Schwarz methods. In T. Chan, T. Kako, H. Kawarada, O. Pironneau (editors), 12th international conference on domain decomposition methods, ddm.org, 2001.

[20] Gander, M. J., Magoules, F., Nataf, F., Optimized Schwarz Methods without Overlap for the Helmholtz Equation. SIAM Journal on Scientific Computing, Vol. 24, No 1, pp. 38-60, 2002.

[21] C. Japhet, F. Nataf, F. Rogier, The Optimized Order 2 Method. Application to convection-diffusion problems, Future Generation Computer Systems, 18(1) (2001), pp. 17-30, Elsevier Science.

[22] Kimn, J.-H., A convergence theory for an overlapping Schwarz algorithm using discontinuous iterates. Numerische Mathematik, 100(1):117–139, 2005.

[23] Lions, P.-L., On the Schwarz alternating method I. First international symposium on domain decomposition methods for partial differential equations, SIAM, Philadelphia, pp. 1-42, 1988.

[24] Lions, P.-L., On the Schwarz alternating method II: stochastic interpretation and order properties. Domain decomposition methods, SIAM, Philadelphia, pp. 47-70, 1989.

[25] Lions, P.-L., On the Schwarz alternating method III: a variant for non-overlapping subdomains. Third international symposium on domain decomposition methods for partial differential equations, SIAM, pp. 47-70, 1990.

[26] Loisel, S., Optimal and optimized domain decomposition methods on the sphere. Ph.D. thesis, McGill University, 2005.

[27] S. Loisel and D. B. Szyld, On the convergence of Algebraic Optimizable Schwarz Methods with applications to elliptic problems. Accepted for publication in Numerische Mathematik, 2009.

[28] Lube, G., Mueller, L., Otto, F.-C., A non-overlapping domain decomposition method for the advection-diffusion problem. Computing, 64:49–68, 2000.

[29] Martin, V., An optimized Schwarz waveform relaxation method for unsteady convection diffusion equation. Applied Numerical Mathematics, 52(4):401–428, 2005.

[30] Mu, J., Solving the Laplace-Beltrami equation on S^2 using spherical triangles. Numer. Methods Partial Differential Equations, 12(5):627–641, 1996.

[31] Nataf, F., Absorbing boundary conditions in block Gauss-Seidel methods for convection problems. Math. Models Methods Appl. Sci., 6(4):481–502, 1996.

[32] Nataf, F., Nier, F., Convergence rate of some domain decomposition methods for overlapping and nonoverlapping subdomains. Numerische Mathematik, 75(3):357–77, 1997.

[33] A. Qaddouri, L. Laayouni, S. Loisel, J. Cote and M.J. Gander, Optimized Schwarz methods with an overset grid for the shallow-water equations: preliminary results, Applied Numerical Mathematics, vol. 58, issue 4, pp. 459–471, 2008.

[34] A. St-Cyr, M.J. Gander and S.J. Thomas, Optimized multiplicative, additive and restricted additive Schwarz preconditioning, SIAM Journal on Scientific Computing, Vol. 29, No. 6, pp. 2402–2425, 2007.

[35] Stanifoth, A. and Côté, J. Semi-Lagrangian integration schemes for atmospheric models – a review. Mon. Wea. Rev., 119 (1991), pp. 2206-2222.

[36] Toselli, A., Widlund, O., Domain Decomposition Methods. Springer, 2004.